SEMIANNUAL REPORT
NASA RESEARCH GRANT NGR-22-011-007

RELIABLE SOLID-STATE CIRCUITS

by

R. E. Bach, Jr.
A. W. Carlson
C. A. Furciniti
R. E. Scott

Electronics Research Laboratory
Northeastern University
Boston, Mass.

July 1, 1965

SEMIANNUAL REPORT

NASA RESEARCH GRANT NGR-22-011-007

RELIABLE SOLID-STATE CIRCUITS

by

R. E. Bach, Jr.
A. W. Carlson
C. A. Furciniti
R. E. Scott

Electronics Research Laboratory
Northeastern University
Boston, Mass.

July 1, 1965

The research reported here covers the period from December 1, 1964 - May 31, 1965, and was sponsored by the National Aeronautics and Space Administration under Research Grant NGR-22-011-007. This report is published for information purposes only and does not represent recommendations or conclusions of the sponsoring agency. Reproduction in whole or part is permitted for any purpose of the United States Government.

RESEARCH STAFF

Ralph E. Bach, Jr., Co-Principal Investigator
Associate Professor of Electrical Engineering

A. William Carlson, Co-Principal Investigator
Senior Research Associate

Charles A. Furciniti
Research Associate

Ronald E. Scott
Dean of the College of Engineering

ACKNOWLEDGMENT

The authors would like to extend their gratitude to Professor William F. King of the Electrical Engineering Department for his cooperation in providing equipment for use in the Grant Laboratory. Special thanks are given to Mr. William Fabrizio for his able service as lab technician and to Miss Martha Wright and Mr. Fabrizio for their enthusiastic and efficient processing of the manuscript.

TABLE OF CONTENTS

FIGURES AND TABLES

I. Introduction

The central theme of the research reported here is the application of advanced circuit concepts for realization of highly reliable and efficient electronic subsystems that meet NASA mission requirements. Such subsystems must be designed for ultimate microminiaturization. To achieve the stated objectives, the research effort during the first six months of the grant period has been directed as outlined in the following discussion.

1.1 System requirements.

Electronic system specifications for NASA spacecraft have been investigated by gathering and examining information concerning mission objectives, system block diagrams and specific circuits for several satellite programs. Of specific help in the continuation of this work is the ready availability of technical documents, which has been made possible by the Scientific and Technical Information Division of NASA. This agency has placed the Northeastern University Library on the initial automatic distribution list for STAR, unclassified NASA formal series reports, and NASA microfiche.

General requirements for electronic systems in space are:

(1) Low power, high efficiency,

(2) Small size, weight,

(3) High reliability.

Requirement (1), above, was significant in the decision to investigate the use of switching techniques for linear power amplification. Requirement (2) leads naturally to the consideration of integrated circuit concepts for system design. Requirement (3), reliability, is of prime importance in any space system realization, and figures significantly in the work reported here and in the future research effort to be made under this grant. Some specific ideas in this regard are discussed in Chapter IV.

1.2 Circuit Development.

Laboratory development of solid-state circuitry concurrent with the above program has been emphasized. A basic effort has involved the use of switching devices to achieve linear power amplification. This technique has the advantage of high efficiency, low distortion and independence of nonlinearities in the active region of the switching device. A full discussion of this work is found in Chapters II and III.

Some experimentation has also been done on a novel scheme for amplitude regulation of an oscillator. The use of a small lamp for oscillator regulation has been

standard practice for some time, but it has been found that the desired regulation can instead be accomplished by the use of a unijunction transistor in a feedback network which should be easily microminiaturized. This circuit application is covered in Appendix B.

1.3 Microminiaturization

The development of integrated circuit techniques has made possible marked improvement in system reliability. Not only have interconnection problems diminished, but it is now apparent that radiation tolerance has improved due to accompanying materials research. Furthermore, it is now feasible to shield complete circuits with only a small increase in weight. Because of the small size of integrated circuits, the structure necessary for support is smaller than that for conventional circuitry and the connector size and number of connections are reduced. All of this leads to a weight saving in the spacecraft with an attendant increase in electronic capability or reduction in vehicle power requirements.

An extensive investigation of the advantages and disadvantages of circuit design for microminiaturization has been carried out. Compatibility with this rapidly advancing technology is a major factor in the design of electronic systems for spacecraft. Some important aspects of microcircuit design pertaining to the electronic systems investigated during this period are discussed in Chapter III.

II. Switching Amplifier Analysis

2.1 Pulse-width modulation (PWM).

In this chapter two schemes for achieving highly reliable linear power amplification are considered and evaluated. In each case investigated, the active devices operate in the switching mode only: power amplification is accomplished by pulse-width modulation. Interest in switching amplifiers is dictated by the following considerations:

(1) High reliability results from the operation of an active device in the switching mode since dissipation is held to a minimum and large parameter variations can be tolerated.

(2) Switching schemes are inherently efficient. In theory, some designs approach 100% efficiency, while in practice, efficiencies in excess of 85% are attainable.

(3) A wide variety of devices, both linear and nonlinear, operating over wide environmental ranges may be used to achieve low-distortion signal amplification. Such circuitry is usually more readily integrated than corresponding linear designs.

Fig. 2.1(a) shows the block diagram of a conventional pulse-width (synchronous) modulator. The signal s(t), added to a triangular wave f(t), modulates the switching time within a period to produce a pulse-width modulated output, y(t). Excellent linearity and low distortion can be obtained provided the signal frequency f_s is much less than the switching frequency f_o [1]. The basic patent for a power amplifier operating in this manner dates back to 1933 [2]. In the preamble of the patent specification, the scheme is presented as an alternative to "arrangements of the prior art" (devices designed to operate in the active region), with the justification that "such arrangements have the inherent disadvantages of large tube losses and low power output for ordinary operating voltages". A later version of the same circuit [3] utilized a sawtooth wave which triggered a Schmitt circuit to produce a pulse-width modulated output.

A simpler scheme for achieving pulse-width modulation, called a two-state modulator, is shown in Fig. 2.1(b). This configuration has been described in a recent paper by Bose [4], although the idea has been in use for many years for pulse-time control of process systems [5]. With RC feedback, symmetrical power supply and hysteresis levels ($\pm$ h, $\pm$ w, respectively), and s(t) = 0, the system output is a square wave. Application of an input signal s(t) modulates the duty cycle and frequency of the pulse output. Such a scheme provides a marked improvement over simple on-off con-

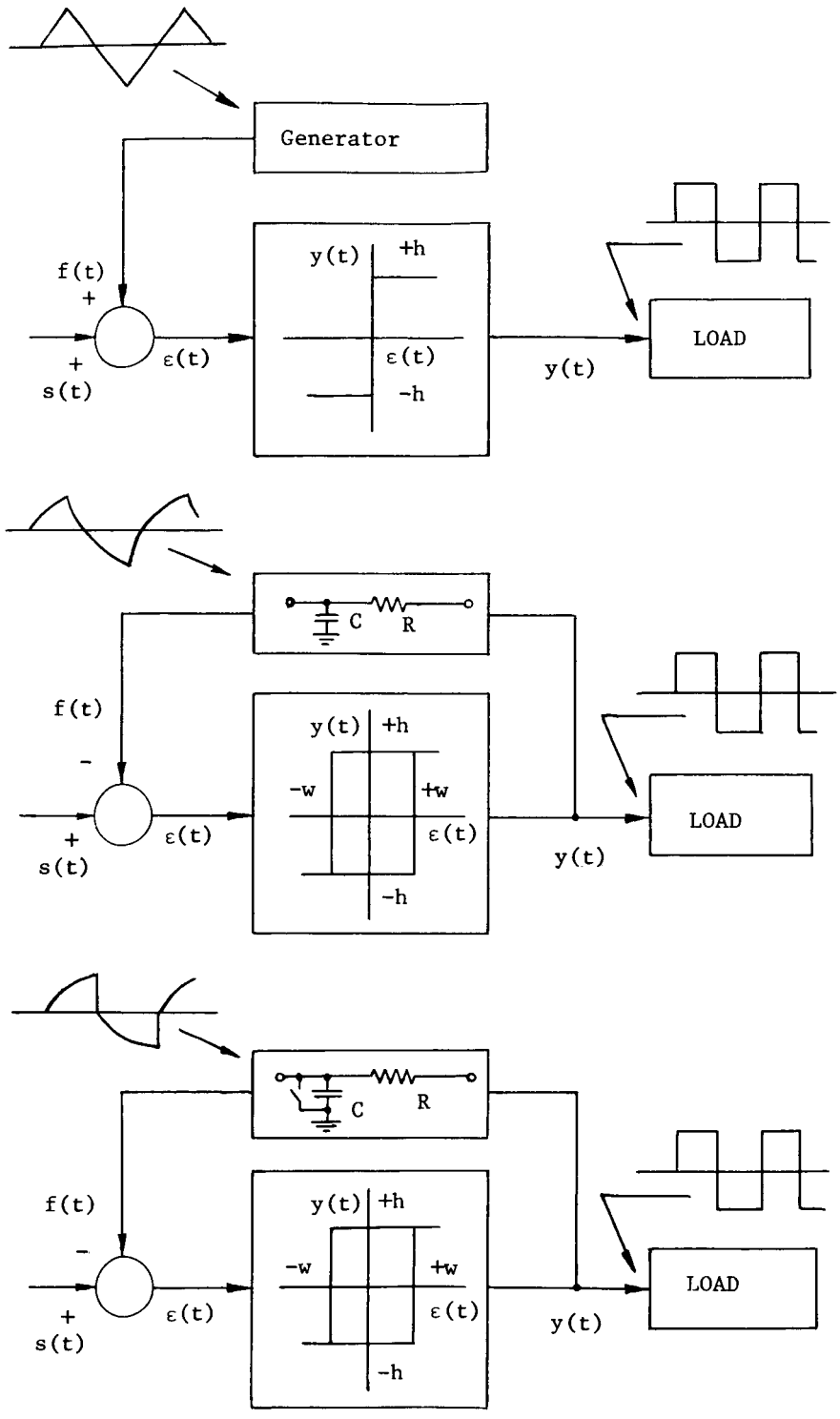

Fig. 2.1 Block diagrams for modulation schemes: (a) pulse-width (synchronous) modulator (b) two-state modulator (c) modified two-state modulator.

trol for process systems and has become widely used.

In Appendix A it is shown that the operation of the two-state modulator with simple RC feedback is equivalent to the modulation of a free-running multivibrator. The circuit exhibits poor linearity due to the exponential nature and the variation in duty cycle of the feedback signal. Since the switching frequency decreases as the signal level increases, 100% modulation is not possible with this system. A significant increase in gain over this design can be achieved by clamping the feedback signal to ground at the start of each switching transition, as indicated in Fig. 2.1(c). This modification allows the inclusion of signal feedback to improve linearity and reduce variation in switching frequency with signal level over the simple RC-feedback case for equivalent power gains. The properties of the two systems are analyzed and compared in the following sections.

2.2 Analysis of PWM Systems.

The self-oscillating PWM systems described in the preceding section may also contain time delay. However, in the analysis that follows, it is assumed that the effect of time delay in the loop is negligible compared to the effect of hysteresis in the switch. Of interest in the analysis will be the period of oscillation

$$T = T_1 + T_2 \quad , \tag{2.1}$$

where T_1 and T_2 are the pulse lengths defined in Fig. 2.2 (note that $T_1 = T_2$ for $s(t) = 0$); the average value $\bar{y}$ of the output waveform $y(t)$, normalized to the power supply level h,

$$Y = \bar{y}/h \quad , \tag{2.2}$$

which can be conveniently written

$$Y = 2T_1/T - 1 \quad , \tag{2.3}$$

as can be determined from Fig. 2.2. Also it will be useful to define the gain

$$G = dY/dX \quad , \tag{2.4}$$

where $X = s(t)/h$ (normalized input signal). When evaluated for $s(t) = 0$, $G = G_o$, which will serve as an approximate small-signal gain expression. Finally, a measure of sys-

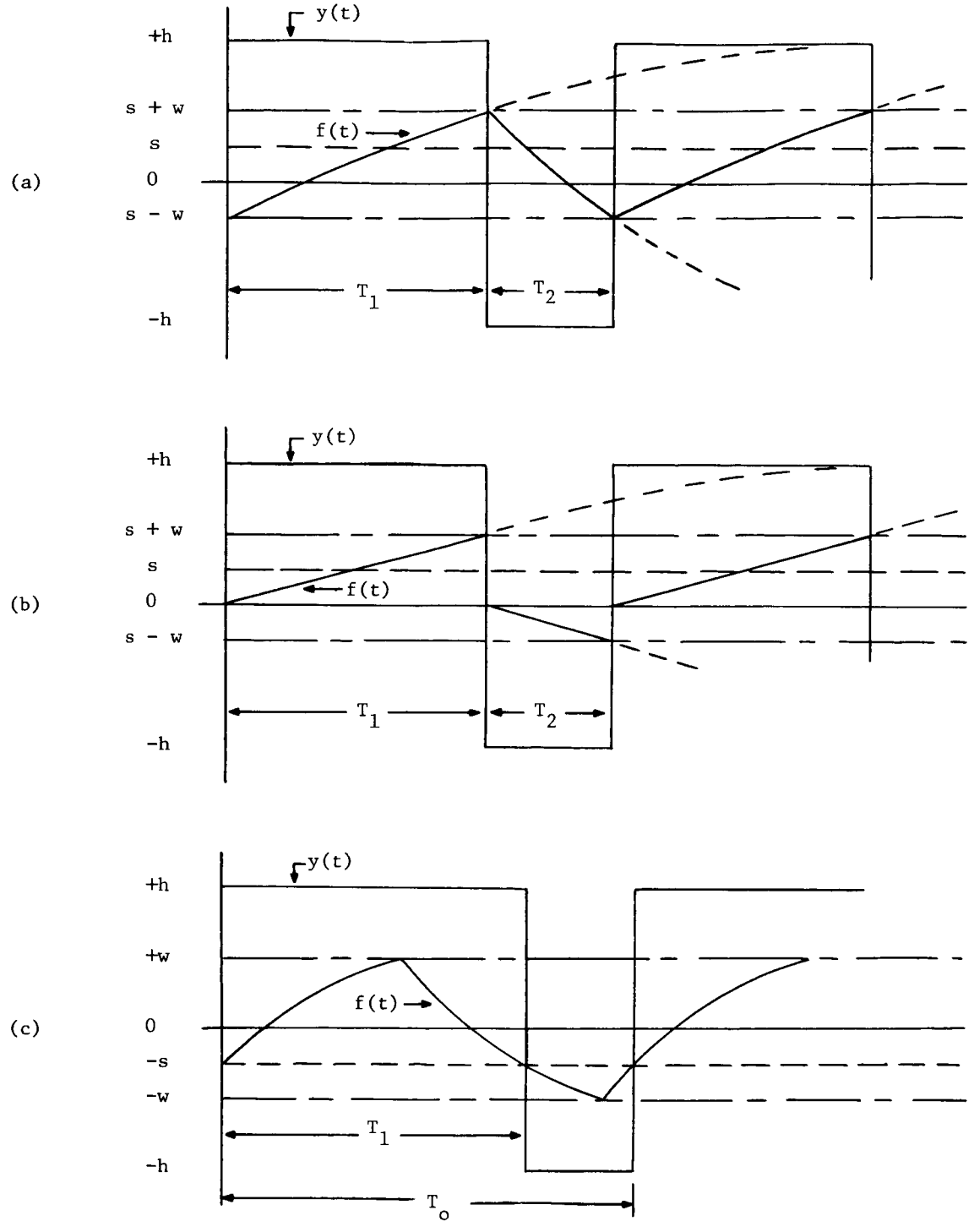

Fig. 2.2 Waveform diagram for modulation schemes: (a) two-state modulator (b) modified two-state modulator (c) synchronous modulator with exponential switching waveform.

tem nonlinearity will be defined as

$$E = (Y - G_o X)/G_o X \quad , \qquad (2.5)$$

a fraction that represents the deviation of the output from its initial slope of G_o. In the analysis that follows, the subscript "a" will be attached to variables in the simple RC-feedback scheme, and the subscript "b" to variables in the switched RC-feedback system.

2.2.1 Simple RC-Feedback.

The simple RC-feedback scheme shown in Fig. 2.1(b) has been analyzed by Bose [4]. These results, using the notation just described are presented here (refer to Fig. 2.2 (a)):

$$T_{1a} = \tau \ln[(1 + W - X)/(1 - W - X)] \quad , \qquad (2.6)$$

where $\tau = RC$ and $W = w/h$ (normalized hysteresis level);

$$T_a = \tau \ln\{[(1 + W)^2 - X^2]/[(1 - W)^2 - X^2]\} \quad . \qquad (2.7)$$

Note that for $s(t) = 0$, (2.7) reduces to the switching period

$$T_o = 2\tau \ln[(1 + W)/(1 - W)] \quad , \qquad (2.8)$$

and that the required hysteresis level for a given T_o/τ is easily found from (2.8) to be

$$W_a = \tanh(T_o/4\tau) \quad . \qquad (2.9)$$

Now, from (2.3), (2.6), and (2.7),

$$Y_a = \frac{2 \ln[(1 + W - X)/(1 - W - X)]}{\ln\{[(1 + W)^2 - X^2]/[(1 - W)^2 - X^2]\}} - 1 \quad . \qquad (2.10)$$

Differentiation of Y_a in (2.10) with respect to X yields, with $X = 0$, the expression for zero signal gain

$$G_{oa} = [2W/(1 - W^2)]/\ln[(1 + W)/(1 - W)] \quad . \qquad (2.11)$$

It should be observed from (2.7) that for full modulation ($X = X_m = 1 - W$), the period T_a is infinite (system not oscillating). For $-X_m \geq X \geq X_m$ the system output remains in the high (or low) state and $Y = \pm 1$. An expression for system nonlinearity at full modulation (worst case) can be obtained by substitution of (2.11) into (2.5) with $Y = 1$, $X = X_m$. Hence:

$$E_{ma} = [(1 + W)/2W]\ln[(1 + W)/(1 - W)] - 1 \quad . \qquad (2.12)$$

2.2.2 Modified RC-Feedback.

A modification of the simple two-state modulator consists of circuitry that causes the feedback voltage to reset to zero each time the output changes state. It will be shown that this system has a higher gain, improved linearity (compared to the previous system having the same hysteresis characteristic), and a smaller change in frequency as a function of the modulating signal. From the waveform diagram for this system shown in Fig. 2.2(b), it can be seen that

$$T_{1b} = \tau \ln[1/(1 - W - X)] \quad , \qquad (2.13)$$

$$T_b = \tau \ln\{1/[(1 - W)^2 - X^2]\} \quad . \qquad (2.14)$$

For $s(t) = 0$, (2.14) reduces to

$$T_o = 2 \tau \ln[1/(1 - W)] \quad , \qquad (2.15)$$

from which

$$W_b = 1 - \varepsilon^{-T_o/2\tau} \quad . \qquad (2.16)$$

The normalized average value of the output can be written, from (2.3), (2.13) and (2.14) as

$$Y_b = \frac{2 \ln[1/(1 - W - X)]}{\ln\{1/[(1 - W)^2 - X^2]\}} - 1 \quad . \qquad (2.17)$$

The derivative of the normalized output with respect to the input, with X = 0, is

$$G_{ob} = [1/(1 - W)]/\ln[1/(1 - W)] \quad . \qquad (2.18)$$

For the switched feedback system it can be seen from (2.13) and (2.14) that when $X = X_m = W$, full modulation occurs, since $T_{1b} = T_b$, and the output level is $Y = 1$. It is interesting to note that the period of oscillation at full modulation is finite. The worst-case nonlinearity figure (full modulation) is obtained as before by substituting (2.18) into (2.5), with $X = X_m$, $Y = 1$. Hence

$$E_{mb} = [(1 - W)/W]\ln[1/(1 - W)] - 1 \quad . \qquad (2.19)$$

2.2.3 Synchronous Operation.

It has been remarked that the two-state modulator with simple RC-feedback exhibits poor linearity due to the exponential nature and the variation in duty cycle of the feedback signal. The duty cycle (and period) variation may be eliminated by supplying the switching signal, f(t), from an external generator as in Fig. 2.1(a). For comparison, however, instead of being a triangular wave, f(t) will be the same as that produced by the feedback system when s(t) = 0. Typical waveforms for this process are shown in Fig. 2.2(c). In addition, the switching period will be set equal to the T_o given by (2.8). Comparison of results obtained from synchronous operation (with exponential switching signal) and operation of the RC-feedback system should then indicate if performance is improved by elimination of the variation in duty cycle.

The operation of the synchronous pulse-width modulator may be explained as follows (refer to Fig. 2.2(c)): when the sum of the input signal s(t) and the switching signal f(t) is positive, the output y(t) is at level + h; when the sum is negative the output is at level -h. With the period T in (2.3) equal to the T_o for a linear feedback system having a normalized hysteresis level W, the analysis yields

$$Y_c = \frac{\ln[(1 + X)/(1 - X)]}{\ln[(1 + W)/(1 - W)]} \quad , \qquad (2.20)$$

for the normalized output and

$$G_{oc} = 2/\ln[(1 + W)/(1 - W)] \quad , \qquad (2.21)$$

for the zero-signal gain.

Now, maximum modulation occurs for $X = X_m = W$, and from (2.5) and (2.21), with $X = X_m$ and $Y = 1$, the expression for maximum system nonlinearity is found to be

$$E_{mc} = (1/2W)\ln[(1 + W)/(1 - W)] - 1 \quad . \qquad (2.22)$$

2.3 Comparison of PWM Systems.

A meaningful comparison between the simple and modified feedback systems can be made by assuming the same hysteresis characteristic for each system. In this case, however, each configuration requires a different ratio T_o/τ, but adjustment of τ allows for operation with the same fundamental zero-signal period T_o. An important characteristic of the modulator with switched feedback is that the period of oscillation does not vary so widely with modulation level. Table 2.1 lists some calculations of the ratio T/T_o for signal levels $X = .9X_m$ and $X = X_m$ for the two systems. Note that T_a/T_o for $X = X_m$ is infinite.

TABLE 2.1

Comparison of period variation with signal level for pulse-width modulation systems.

W	T_a/T_o $X = .9X_{ma}$	T_b/T_o $X = .9X_{mb}$	T_a/T_o $X = X_{ma}$	T_b/T_o $X = X_{mb}$
.1	3.19	1.05	∞	1.06
.2	2.50	1.13	∞	1.15
.3	2.12	1.22	∞	1.29
.4	1.89	1.44	∞	1.57

Table 2.2 summarizes calculations of gain and nonlinearity made for the worst case, $X = X_m$ (full modulation). It is seen that nonlinearity (as defined in (2.5)) with switched feedback is about one-half that for the linear feedback system. This result is somewhat deceiving since the gain of the modified system is significantly higher. If signal feedback is added to this system to reduce the gain G_o to that of the linear feedback system for each value of W, nonlinearity figures and period variation are reduced considerably. The results of digital computer calculations are best

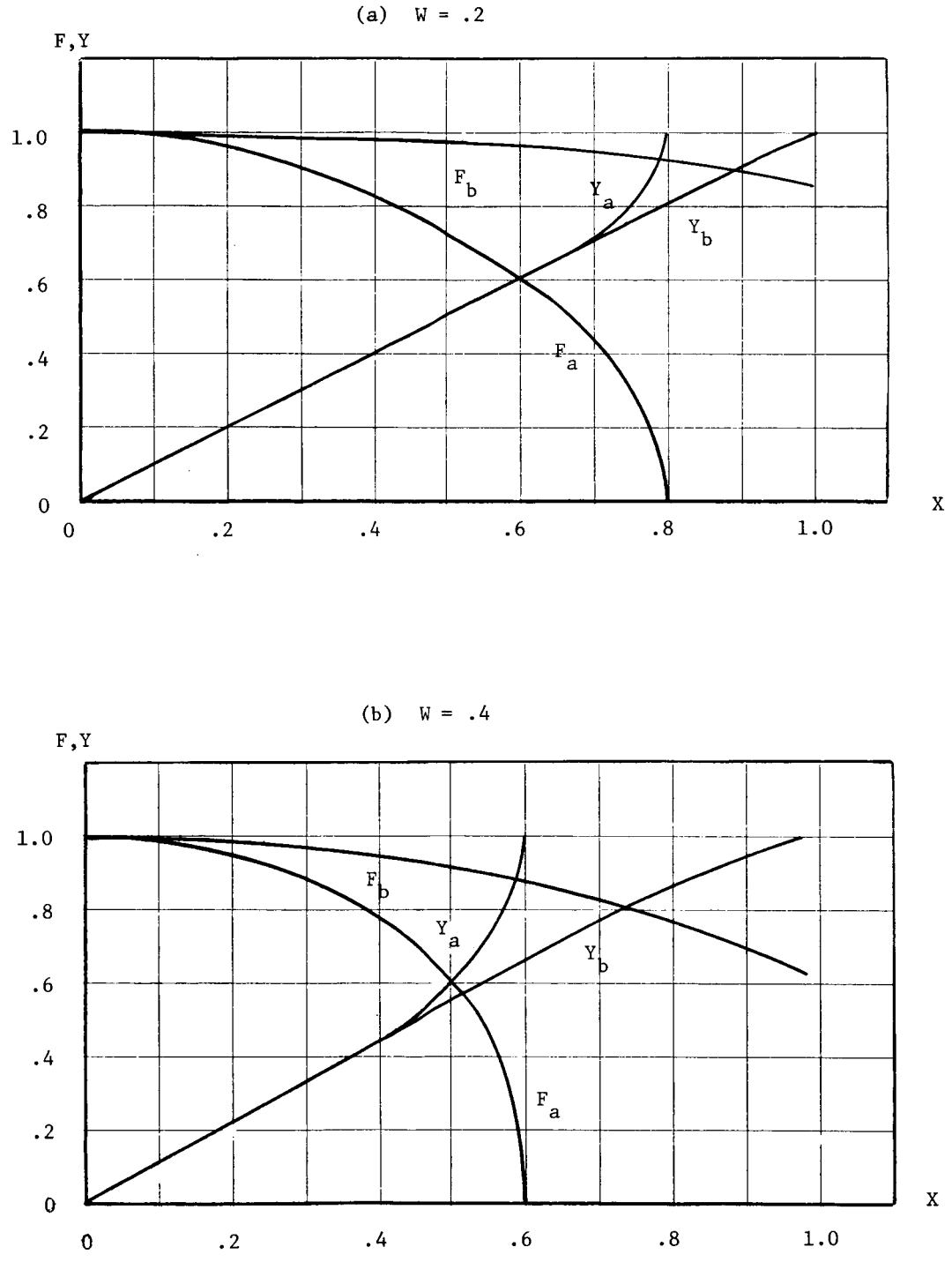

Fig. 2.3 Normalized average output and switching frequency versus normalized input for two-state modulator (Y_a, F_a) and modified two-state modulator (Y_b, F_b) with signal feedback for equivalent power gain, for (a) W = .2, (b) W = .4.

TABLE 2.2

Comparison of zero-signal gain and nonlinearity at full modulation for pulse-width modulation systems

W	G_{oa}	G_{ob}	G_{oc}	% E_{ma}	% E_{mb}	% E_{mc}
.1	1.01	10.6	9.97	9.4	5.5	0.2
.2	1.03	5.60	4.93	21.5	10.8	1.2
.3	1.06	3.99	3.23	34.5	16.5	3.2
.4	1.12	3.26	2.36	48.8	23.1	5.9

shown by the graphical comparison illustrated in Fig. 2.3 for typical hysteresis levels. A significant improvement in linearity, dynamic range and frequency stability can be observed with the modified RC feedback system.

Calculations for synchronous operation are shown in Table 2.2 in columns headed G_{oc} and % E_{mc}. It should be recognized that the zero-signal switching waveform is the same as that produced by the corresponding simple RC-feedback system. Gain is significantly higher, being nearly as high as that given for the switched feedback case. The nonlinearity figures are much lower than either of the two feedback schemes. It is interesting to note that in a synchronous system deviations from linearity due to a nonlinear switching waveform tend to be minimized when that waveform is made up of equal, symmetrical rising and falling segments. This is an important fact when the relative complexity of generation of a linear sawtooth is considered.

To summarize, it has been shown that performance of a simple two-state pulse-width modulator can be improved considerably by use of a modified feedback network. However, the properties of a synchronous modulator are the best of the three types, even with an exponential switching signal. There is, of course, no shift in switching frequency with input signal and a very high degree of modulation is obtainable.

III. Switching Amplifier Design

During the first six months of this grant several practical switching amplifiers were designed and evaluated. In the following discussion the switching amplifier is considered in two sections: (a) a switching circuit that creates a two-state pulse-width modulated (PWM) signal from the low frequency input s(t), and (b) the power stage that amplifies the two-state PWM signal and drives the low-pass load. A block diagram of the amplifier and test apparatus is shown in Fig. 3.1.

In order to present a meaningful comparison of the switching schemes employed, the power stage, supply levels and load were the same in each configuration. The maximum power obtainable from this amplifier is about two watts. The value is determined from

$$P = [V_{cc} - V_{ce}(SAT)]^2/2R_L \quad , \qquad (3.1)$$

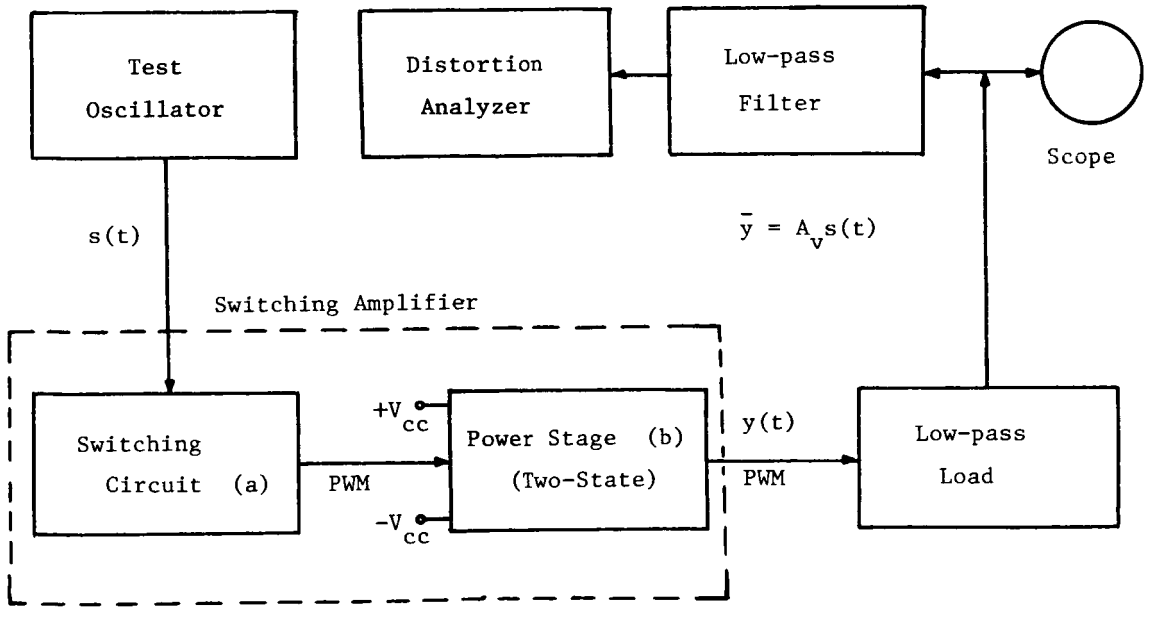

Fig. 3.1 Switching amplifier test configuration.

where:

V_{cc} = 15 volts (power supply voltage),

$V_{ce}(SAT) \simeq 0.3$ volts (output transistor saturation drop),

R_L = 50 ohms (resistive component of load).

Considerable design effort was expended in attempting to maximize voltage gain (A_v), power gain (A_p), efficiency and gain linearity. Careful attention was given to such performance criteria as step response, overload recovery, temperature stability and output distortion (including IM distortion). The results of this work are quite promising and indicate that a switching amplifier can be used as an efficient driver for the following loads:

(a) Gimbal torquers
(b) Accelerometer coils
(c) Gyro wheels
(d) Gyro heating elements
(e) AC and DC servo motors
(f) Tape recorder heads
(g) Loudspeakers
(h) Relays and solenoids.

3.1 Power Stage Considerations.

The design of power stages for linear amplification is well documented in the literature. However, the performance of linear power stages suffers from an efficiency limitation. One of the major advantages of the use of switching amplifiers is the high efficiency inherently obtainable. Consider the complementary (two supply) power amplifier of Fig. 3.2: here only 0.3 volts ($V_{ce}(SAT)$) out of the 15 volt supply does not appear across the load. This represents only a 2% reduction in efficiency. If high speed power transistors are used, active-region switching losses can be kept below 10% of the rated power output. Associated power-stage circuitry contributes about a 10% loss, and, if switching circuit losses are below 10% an overall efficiency in the neighborhood of 75% can be obtained. This figure is significantly higher than the practical efficiency attainable with a class B linear amplifier.

If only one power supply is available the complementary design is easily modified into a bridge configuration. (See Fig. 3.3).

3.1.1. Problems of Driving an Inductive Load.

For many important practical applications of the switching amplifier the load

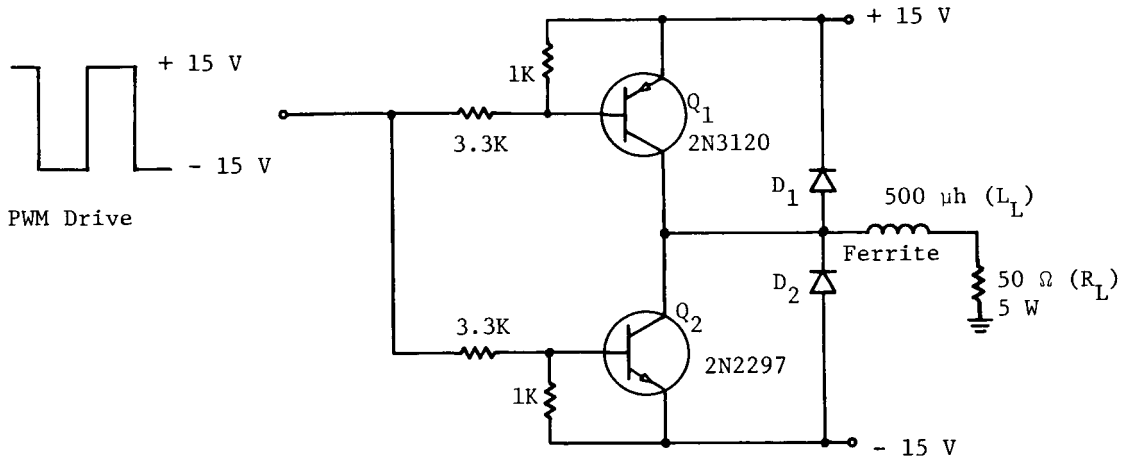

Fig. 3.2 Complementary two-state power stage.

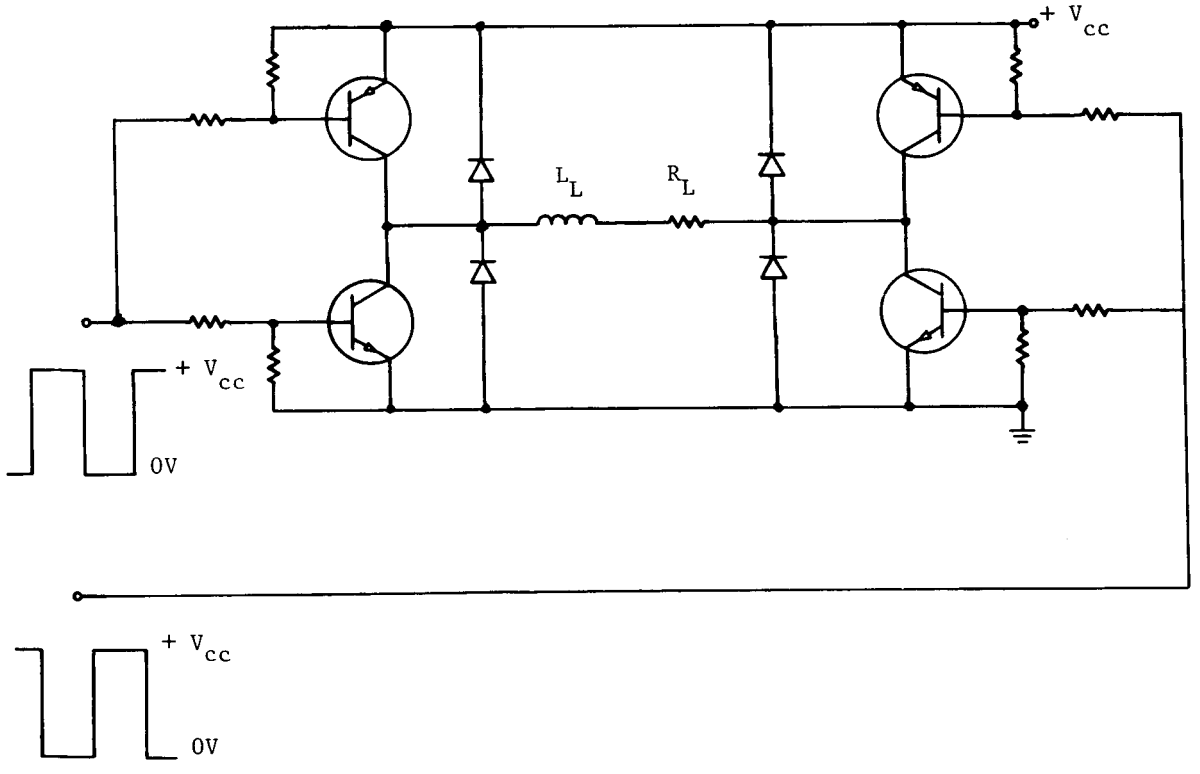

Fig. 3.3 Complementary bridge configuration.

must be inductive. A word of caution is in order concerning magnetic material in the load. Most iron is quite lossy at high frequency. However, eddy current losses at the switching frequency can be virtually eliminated if ferrite is used instead of iron laminations.

The inductive load acts as a low-pass filter. However, the induced voltage across the inductor at the instant of switching could destroy the output transistors. To prevent this two clamp diodes (D_1 and D_2 of Fig. 3.2) were added to the power stage. Fig. 3.4(a) shows the waveforms of the output drive and the load (ripple) voltage for a 50% duty cycle PWM input. When the input duty cycle is other than 50%, most of the load current flows in one direction. Fig. 3.4(b) shows the effect on the output waveform.

It should be pointed out that the speed of the output transistors must be high to minimize the large currents which flow because of the differences in the turn-on and turn-off times. During a transition both output transistors can be on for a time equal to this difference.

3.1.2 Choice of Switching Frequency.

Because the switching frequency limits the useful bandwidth of the amplifier it should be chosen as high as possible consistent with the frequency response of the power transistors. For example, if the output transistors have an f_T = 100 mc and h_{fe} = 50, then $f_\beta \simeq$ 2mc. This figure corresponds to an output rise time of about 0.17 μs, based on a first-order step response. During this time the transistor is operating within its active region. In order to minimize the overall effect of high dissipation in the active region, the period of the output should be chosen at least ten times greater than 0.34 μs (two transitions per period), which corresponds to a maximum switching frequency of nearly 300 kc.

Transistors capable of switching the currents associated with a 2 watt load can be made in either discrete or monolithic form, with saturation resistances of less than 2 ohms. This, of course, represents most of the output impedance of the amplifier.

3.1.3 Amplifier Bandwidth.

The useful bandwidth of an amplifier with f_o = 300 kc (zero-signal switching frequency) can not be determined until the frequency change with input is considered. This change for a typical two-state modulator could lower the switching frequency to about 100 kc at 90% modulation (See Chapter II).

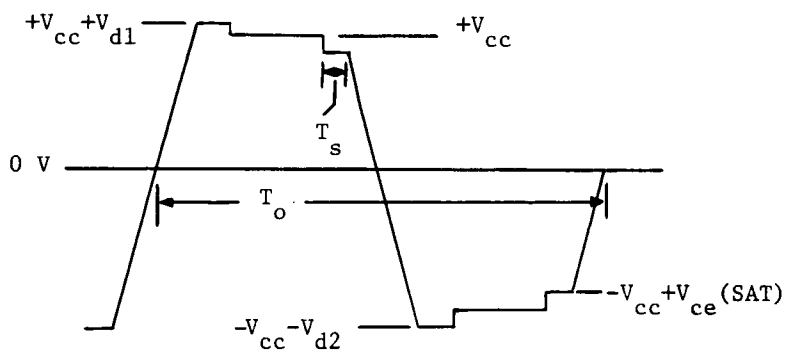

Output Drive

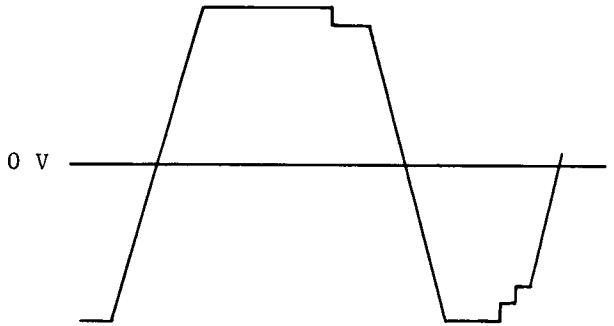

Output Drive

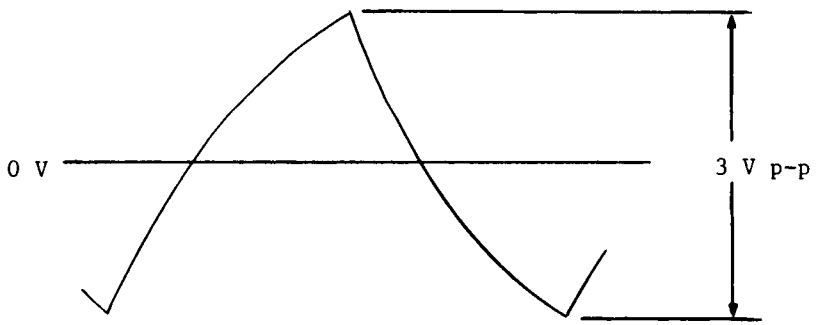

Output Ripple

(a)

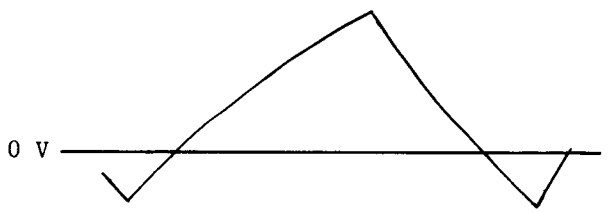

Output Ripple

(b)

Note: V_d = 0.7 V (diode drop)
V_{cc}(SAT) = 0.3 V (saturation)
V_{cc} = 15 V (power supply)
$T_r = T_f$ = 0.1 µs (rise and fall time)
T_o = 4 µs (period at 50% duty cycle)
T_s = 0.2 µs (storage time)
L/R = 10 µs (load time constant)

Fig. 3.4 Power stage output waveforms.

Distortion figures given in Reference [1] pertain to the presence of difference frequencies between harmonics of the input signal and the switching frequency that fall within the amplifier band. To keep distortion from this cause within 1%, a ratio of about 6 to 1 between the lowest switching frequency and amplifier cut-off frequency should be observed. Hence, the useful amplifier bandwidth should be about 17 kc. The time constant of the inductive load was adjusted accordingly. It should be pointed out that the distortion just mentioned is not the same as the harmonic distortion caused by a nonlinear gain characteristic. This latter distortion is normally much larger and will subsequently be considered.

The ripple current in the load resistor is quite large because only a 6 db/octave roll-off is provided by the single L-R combination. Reference to Fig. 3.1 shows a low-pass filter between the load resistor (R_L) and the distortion analyzer expressly for the purpose of eliminating ripple from the measurements.

3.1.4 Overload and Step Response.

Any attempt at overmodulation of the switching amplifier results in hard limiting, i. e., switching action ceases and the output remains in one state or the other for the duration of the disturbance. Overload recovery time is a function of the propagation and storage delays of the transistors because there are no large energy storage devices requiring discharge time. Similarly, the step response for a small signal input reflects the delay time of the amplifier, and has rise and fall times dictated by the L-R time constant of the load.

3.2 Self-Oscillating Switching Amplifiers: Hysteresis Type.

The analytical discussion presented in Chapter II concerns a two-state modulator with hysteresis and RC feedback. A self-oscillating system operating in this mode was constructed for evaluation. A block diagram of the system is shown in Fig. 3.5.

A schematic of the Schmitt trigger used is shown in Fig. 3.6. An important consideration in the operation of the circuit is that a 2N706 transistor is used as a 6 volt zener diode. The base-emitter breakdown is very sharp and no "keep alive" current is required.

The output of the Schmitt circuit is inverted by Q_3 and fedback through an RC network. The switching frequency is determined by the RC time constant and the hysteresis characteristic of the Schmitt. If the trigger input is properly biased, the output is a square wave for $s(t) = 0$.

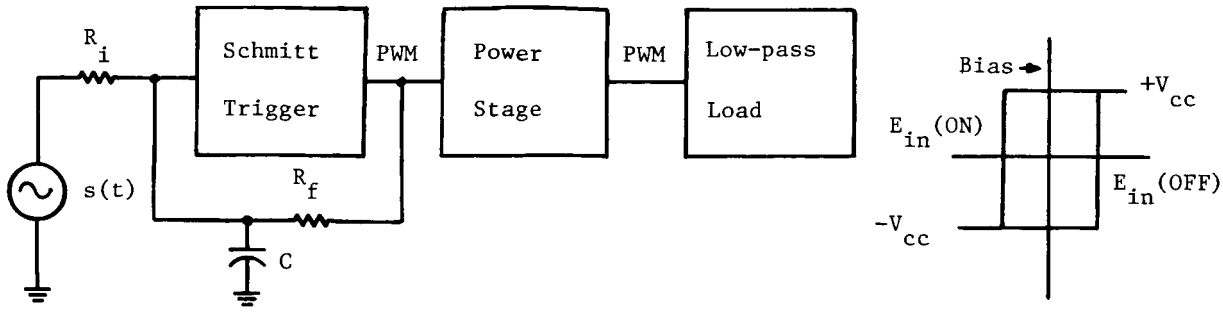

Fig. 3.5 Self-oscillating modulator (hysteresis type).

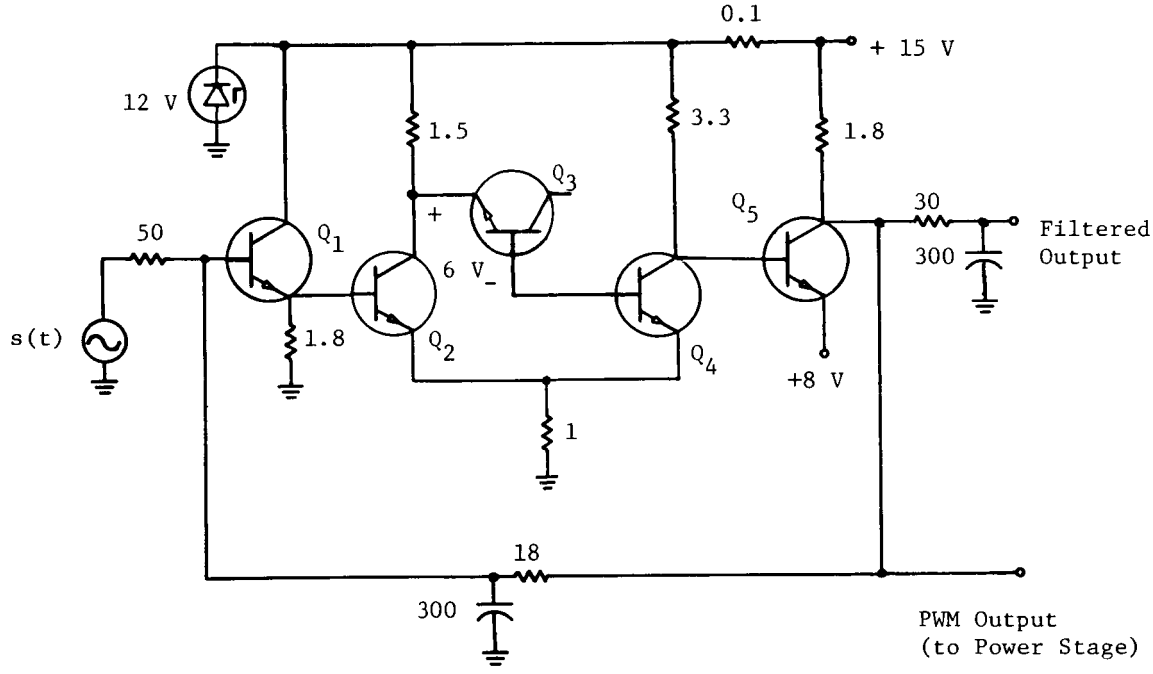

Note:

1) All resistor values in kilohms

2) All capacitors in pico-farads

3) All transistors - 2N706

Fig. 3.6 Self-oscillating switching circuit (hysteresis type).

3.2.1 Stability Considerations.

Since the switching amplifier is direct coupled, the DC operating conditions must be carefully controlled. The two trigger levels of the Schmitt circuit shown in Fig. 3.6 are given by the following expressions:

$$E_{in}(ON) = [V_{cc} - V_{ce}(SAT)]R_E/(R_E + R_2) + V_{be1} \quad , \qquad (3.2)$$

$$E_{in}(OFF) = \frac{V_{cc} - V_{ce}(SAT)}{(R_1 + R_E)(\beta_{SAT} + 1)} \left[R_s + \frac{R_E R_1}{R_E + R_1}\right] + \frac{V_{be1}R_1 + R_E(V_{cc} + V_{bc})}{R_E + R_1} \quad . \qquad (3.3)$$

The base-emitter diodes of the transistors used in the Schmitt have a -2.5 mv/°C temperature coefficient. Stabilization of the firing levels given by (3.2) and (3.3) can be accomplished over a temperature range in excess of 100° C, by using a 12 volt zener (+6 mv/°C temperature coefficient) and by choosing R_1, R_2, and R_E correctly.

The two firing levels for the circuit shown are 5.6 V (ON) and 4.4 V (OFF). The output of Q_5 swings between + 15.0 V and + 8.8 V. Both of the power-supply levels are assumed to be temperature stable. The feedback waveform must be centered around + 5.0 V (Bias in Fig. 3.5) in order to obtain a square-wave output with no input. This bias is provided by R_f and R_i in combination with R_{in}, the input impedance seen at the base of Q_1.

3.2.2 Gain and Distortion.

In the hysteresis amplifier a DC input of 5.6 V produced 90% modulation in the PWM output waveform. If the Schmitt circuit drives a power stage similar to the one shown in Fig. 3.2 between $\pm$ 15 V, and if $V_{ce}(SAT)$ = 0.3 V the DC output voltage (after low-pass filtering) for m = 0.9 (modulation level) would be

$$\bar{y} = m[V_{cc} - V_{ce}(SAT)] = 13.2 \text{ V} \quad . \qquad (3.4)$$

The corresponding voltage gain is

$$A_v = \bar{y}/s = 2.4 \quad . \qquad (3.5)$$

The measured harmonic distortion in the output for s(t) = 5.6 V RMS was 4.8% occurring mostly as 3rd and 5th. This relatively high distortion could be lowered by sacrificing gain through additional signal feedback. A substantial amount of feedback exists through the same RC network that generates the switching waveform. These results are compared to other switching amplifier systems in Table 3.2.

3.2.3 Efficiency.

By carefully selecting the bias resistors it was possible to run this amplifier with 85% efficiency at full load. The zero-signal (standby) power drain was 0.3 watts which was principally due to the power taken by the drive circuit of the output transistors. This circuit then represents a practical realization of the efficiency figures discussed in section 3.1.

3.3 Self-Oscillating Switching Amplifiers - Delay Type.

A simple realization of a self-oscillating switching amplifier is shown in Fig. 3.8 (including power stage). The basic amplifier has an input deadband characteristic, although the inductive load and the output diodes keep the output pulse waveform from switching to the zero level. The amplifier also has a significant time delay of approximately 0.6 μs. The zero-signal switching frequency therefore depends on the input switching levels (+ V_{be1}, - V_{be2} in Fig. 3.7), the time delay (T_d) and the RC-time constant in the feedback network.

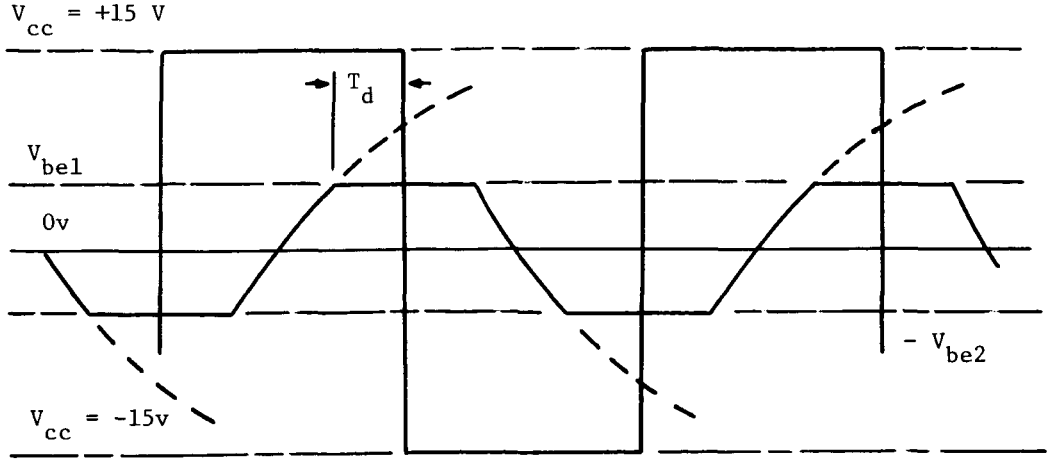

Fig. 3.7 Output and summed waveforms.

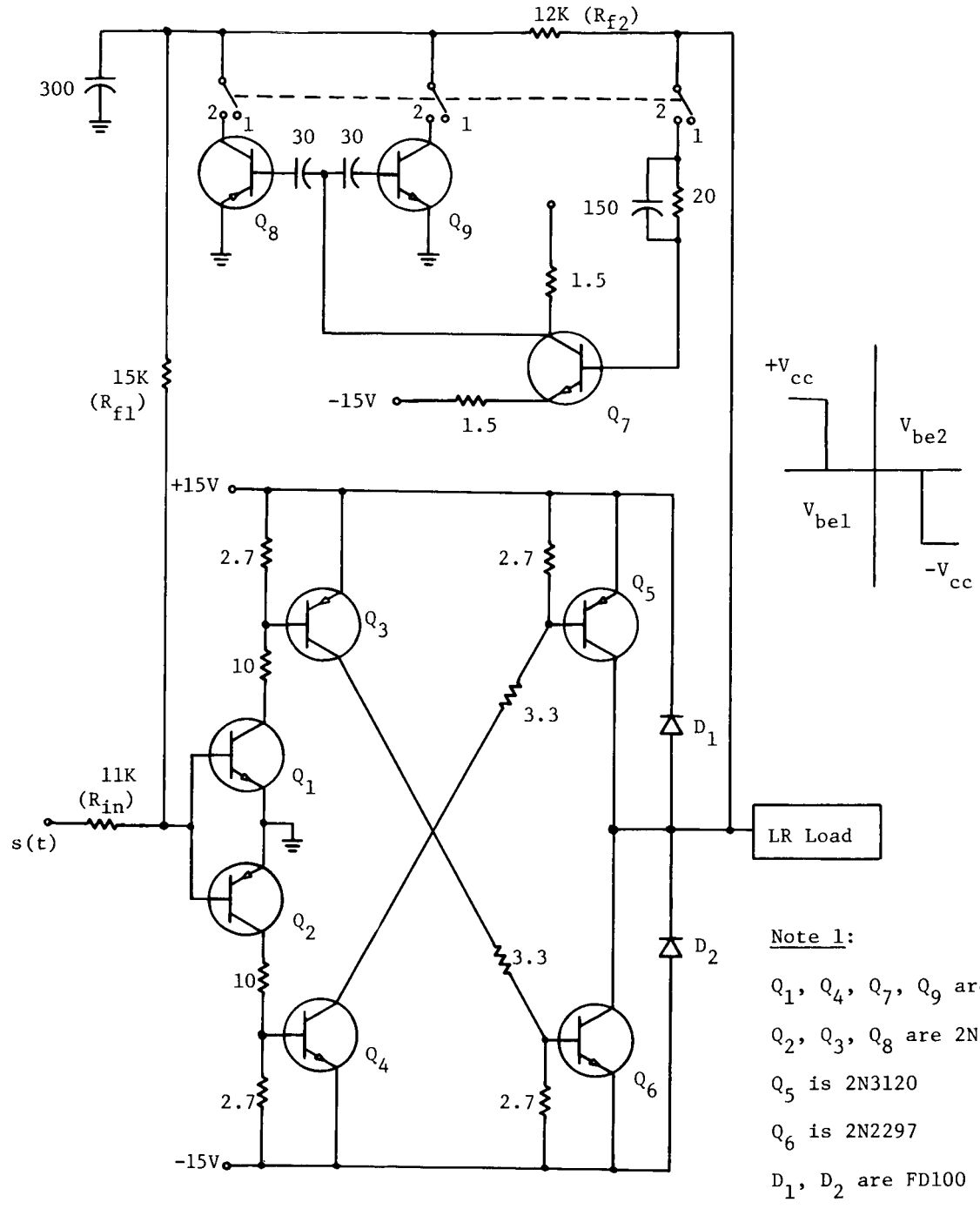

Note 1:

Q_1, Q_4, Q_7, Q_9 are 2N706

Q_2, Q_3, Q_8 are 2N976

Q_5 is 2N3120

Q_6 is 2N2297

D_1, D_2 are FD100

Note 2:

All resistors in kilohms

All capacitors in picofarads

Fig. 3.8 Self-oscillating modulator (delay type) with switched RC feedback.

Analysis of operation is somewhat more complicated than that for the models described in Chapter II. However, overall operation is sufficiently similar so that it was decided to try the switched feedback scheme and also to operate the amplifier as a synchronous modulator. The results are described below.

3.3.1 Stability Considerations.

Careful examination of the circuit presented will show that the V_{be} drops of Q_1 and Q_2 must be matched and must track with temperature. Since these levels represent the switching points of the amplifier any unbalance will cause a DC output to exist.

There is an obvious DC problem due simply to the fact that the output transistors (one NPN and one PNP) can have considerably different saturation drops. Careful attention must be paid to selecting reasonably matched types. The 2N2297 and 2N3120 have a V_{ce}(SAT) of 0.2 V and 0.3 V respectively at 200 ma. The difference voltage represents a very small percentage of the full output.

3.3.2 Gain and Distortion.

With the switch in position 1 the circuit of Fig. 3.8 takes the form of a two-state modulator with simple RC feedback. For this system, when the sum of the feedback signal f(t) and the input signal s(t) reaches the level V_{bel}, Q_1 turns on, effectively clamping the waveform (See Fig. 3.7). Because of the propagation delays the output stage switches T_d seconds later. With a time constant of τ = 2.8 μs in the feedback path the zero-signal switching frequency is 250 kc, which decreases to 140 kc at a 90% modulation level. This characteristic of the two-state modulator has been discussed previously. Voltage gain and distortion at the 90% modulation level (sinusoidal input) are 1.8 and 1.6%, respectively.

The advantages of modifying the exponential feedback signal by clamping to ground at the start of each output transition have been discussed in Chapter II. A practical circuit for accomplishing the clamping is shown in Fig. 3.8, with the switch in position 2. The PWM output is coupled to an inverter, differentiated and fed to PNP and NPN transistors in parallel across the capacitor in the RC feedback network. For a small fraction of the time constant either one of the two transistors (depending upon the polarity) closes to ground to provide the desired clamping effect. As can be observed from the results shown in Table 3.2, the fractional decrease in switching frequency from f_o is greater with the modified feedback scheme, contrary to what is predicted by the analysis of Chapter II. The gain is higher, as expected, but so is the

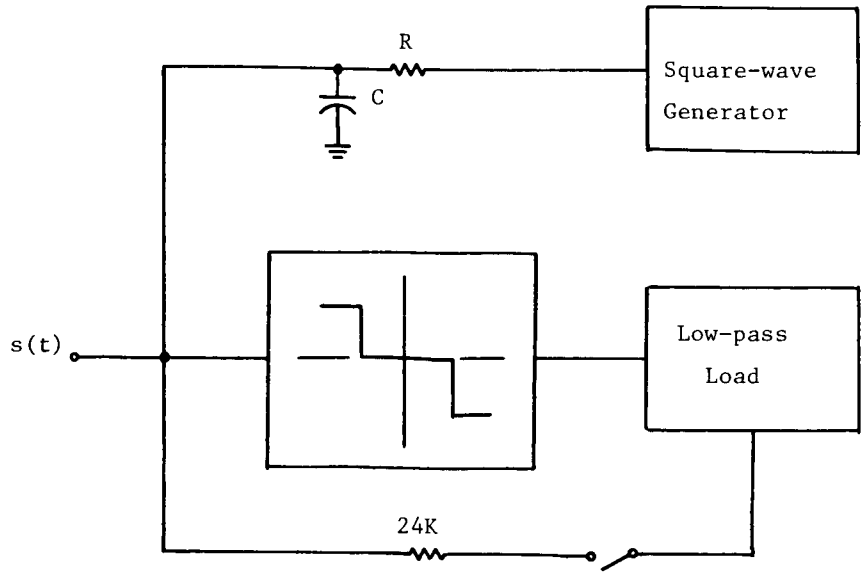

Fig. 3.9 RC Synchronous modulator.

distortion figure. However, measurements were not made for the same zero-signal switching frequency, and, it should be noted, the mathematical model of this switching amplifier is not as simple as the one discussed in Chapter II. Some further analytical and experimental work in this area is anticipated.

In an effort to measure the open-loop characteristics of the amplifier, the feedback connection from the amplifier output was opened and a square-wave generator of the same f_o and amplitude as produced in the simple RC case was substituted as the drive for the RC network. (See Fig. 3.9). The voltage gain increased substantially because the signal feedback path was eliminated. The distortion also increased, and at 90% modulation was found to be 5.7%. However, after the gain was reduced to the same value as before by separate signal feedback through the 24K resistor in Fig. 3.9, the total distortion dropped to 1.5%. This distortion is completely attributable to nonlinearities in the gain characteristic since the switching frequency is fixed by the generator.

In the open-loop configuration, the gain A_{vo},(not including input attenuation), was measured to be 6.85 for small-signal input. With this figure it should be possible to predict the gain for the simple RC - feedback case from the formula

$$A_v = \alpha A_{vo}/(1 + \beta A_{vo}) \quad , \qquad (3.6)$$

where $\alpha = R_f/(R_{in} + R_f)$, $\beta = R_{in}/(R_{in} + R_f)$ and $R_f = R_{f1} + R_{f2}$, as shown in Fig. 3.8. For values of R_{in} = 11 K and R_f = 27 K, A_v = 1.76, which compares favorably with the measured value of 1.8.

3.3.3 Thresholding.

An advantage of using an amplifier with a deadband characteristic (See Fig. 3.8) is that a mode of operation called thresholding is possible. When the amplifier is first turned on, the output is at zero volts and there is no feedback to start the switching. All transistors are biased off and the power drain is practically zero. Switching action does not begin until the signal is raised to a level equal to $V_{be}(R_f + R_{in})/R_f$. By properly designing the feedback path (i. e., making R_f large) it is possible to have switching cease when the input drops below a prescribed level, thereby constraining the operation so that the standby power drain is virtually zero.

3.4 Open-Loop Switching Amplifier.

Because the performance of a synchronous system with separate signal feedback was superior to the other approaches tried, considerable time was spent on a design having the following performance criteria:

(a) Voltage gain > 15

(b) Distortion ≈ 1% at full modulation

(c) Wide temperature range

(d) Feasible for microcircuit construction

(e) Good transient and overload recovery.

An amplifier designed to these specifications is shown in Fig. 3.10.

3.4.1 Selection of Switching Waveshape.

The use of a separate oscillator required in a synchronous system allows an improvement in gain linearity and distortion because the generation of a linear sawtooth switching waveform is possible. The design of a sawtooth generator operating at 200 kc was dictated by the state of the art in microcircuit technology. For example, the use of capacitance larger than a few hundred picofarads or resistors in excess of 10 kilohms is undesirable. The design is further restricted because no practical inductance is available in microcircuit monolithic construction and only small values are permissible in hybrid construction.

A design suitable for realization in microcircuit form utilizes a standard Schmitt-trigger circuit with feedback, employing a Miller integrator to multiply the time constant of a small RC (See Fig. 3.10). This circuit yields a sawtooth of better than 1% linearity up to + 80° C and performs satisfactorily to a temperature of + 120° C. The sawtooth waveform and the PWM output levels are shown in Fig. 3.11. The circuit is sure starting and component variations within the range of practical microcircuit limitations (i. e., ± 20% resistors, ± 20% capacitors) show up only as changes

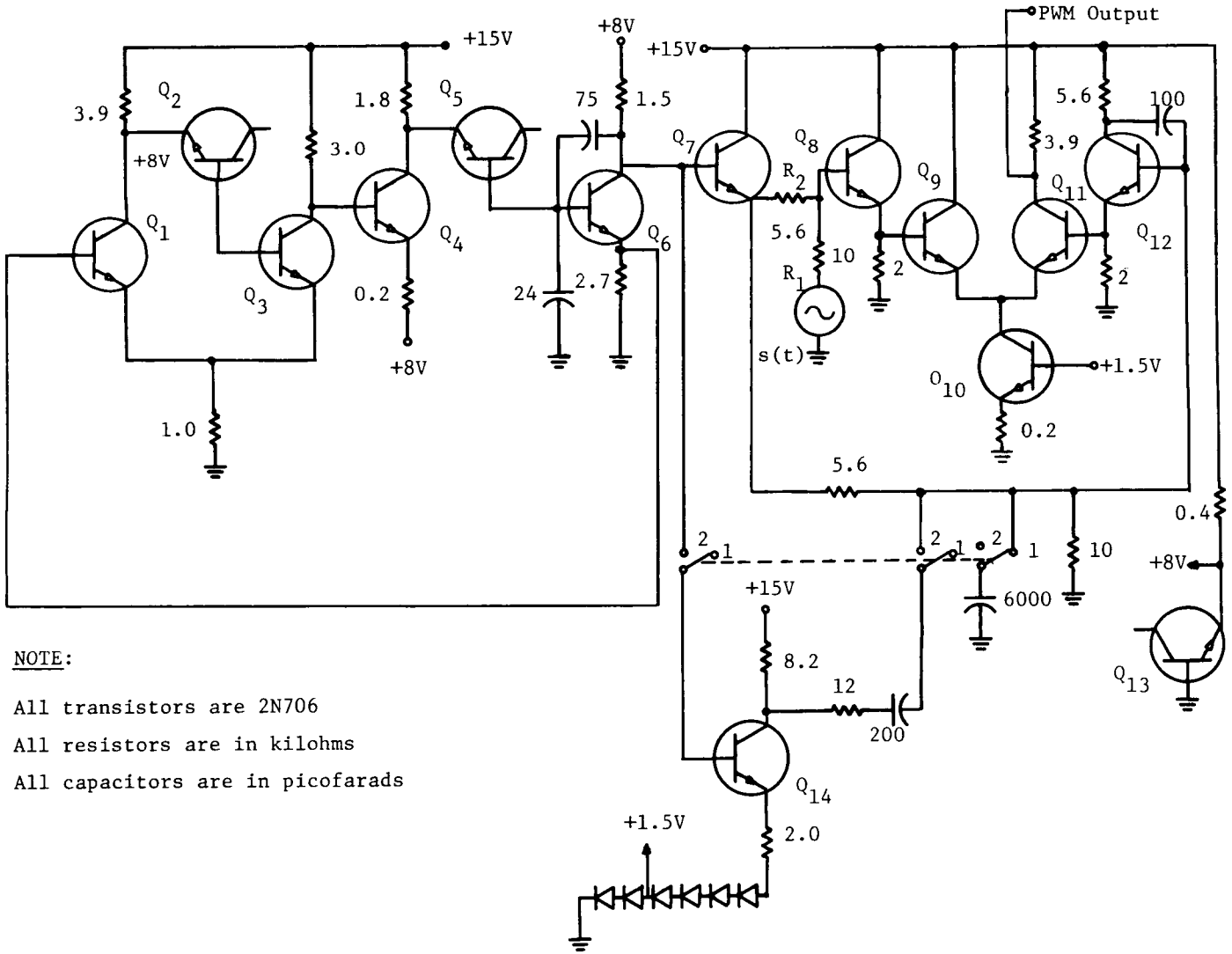

NOTE:

All transistors are 2N706

All resistors are in kilohms

All capacitors are in picofarads

Fig. 3.10 Synchronous modulator (sawtooth).

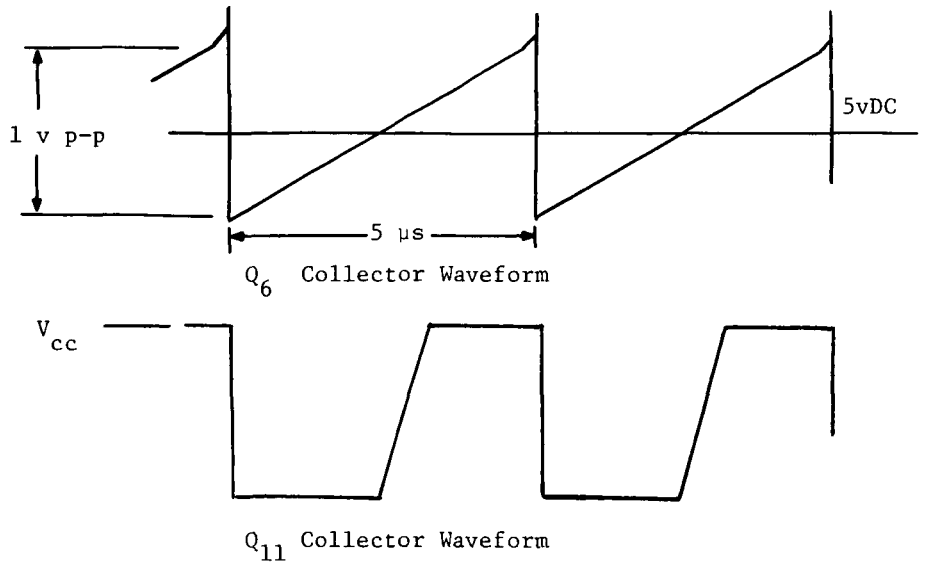

Fig. 3.11 Sawtooth and PWM output signals.

in the initial frequency. This represents no serious limitation in performance.

Shaping of the input-output characteristic of a switching amplifier to some functional specification (e. g., logarithmic) should be possible by properly shaping the switching waveform. A nonlinear sawtooth is probably the most practical waveform for this purpose. This aspect of switching amplifier performance is yet to be investigated.

3.4.2 Differential Amplifier.

In order to provide the highest gain, the hysteresis of the crossover detection circuit (trigger circuit) should be very small, as should the amplitude of the sawtooth. With this in mind, a high gain differential amplifier was designed. The input change (at sawtooth terminals) required to move the output transistor from saturation to cut-off is 0.1 V. If the transition time is limited to 10% of the period, the minimum sawtooth amplitude must be 1.0 V (peak-to-peak).

The reference level for the differential amplifier is obtained by RC filtering the sawtooth to insure the same DC level on both sides regardless of the temperature change. Another approach to obtaining the reference level, more compatible with micro-circuit design requirements, is shown in Fig. 3.10 with the switch in position 2. Since no large L's or C's are permitted, the removal of the sawtooth is accomplished by inverting it and summing the inverted waveform with the original (hum bucking). The resulting ripple in the linear range of the waveform was reduced to less than 50 mv p-p, but even this was enough to increase the distortion significantly. A small amount of

additional filtering is accomplished by using the first transistor stage on the reference side of the differential amplifier as a modified Miller integrator, but more work is required on this approach before it becomes useful.

3.4.3 Gain and Distortion.

The voltage gain of the synchronous system (including the power stage) is given by

$$A_{vo} = 2(R_2/R_1)[V_{cc} - V_{ce}(SAT)]/z(t) \quad , \qquad (3.7)$$

where z(t) is the peak-to-peak sawtooth amplitude; and the power gain by

$$A_p = A_{vo}^{\ 2} R_{in}/R_L \quad . \qquad (3.8)$$

For the values of $R_{in} \simeq 15$ kilohms, $R_L = 50$ ohms, $R_1 = 10$ kilohms, $R_2 = 5.6$ kilohms, the gains are $A_{vo} \simeq 16.5$ and $A_p = 50$ db.

The power drain of the switching amplifier alone is less than 1/4 watt. The gain is as stable as (a) the power supplies and (b) the peak-to-peak level of the sawtooth. The sawtooth amplitude is as stable as the trigger points on the Schmitt, and it has been previously pointed out that these trigger points can be compensated for temperature changes.

It was not possible to 100% modulate this system without flattening one side of the output sine wave because of the small spike occurring on the end of the sawtooth. The resulting output waveform is shown in Fig. 3.12. The distortion was measured by low-pass filtering the differential-amplifier collector waveform at a 90% modulation level. The measured value for total harmonic distortion was 1.2%. A second test was performed using equal inputs of 500 cps and 2000 cps. With the filtered output just below the flattening level no IM distortion was detectable.

Table 3.2 summarizes frequency, gain and distortion measurements for all of the amplifier designs presented in this chapter.

3.5 Microcircuit Power Considerations.

If a hybrid construction for a microcircuit is considered, there is little problem with the output stage in either the complementary push-push or bridge form. PNP transistors can be attached to the same inert host material as the NPN types.

The problems are much more difficult if a monolithic microcircuit is desired.

Fig. 3.12 Modulation limits of PWM output

Here, PNP transistors can not (without great difficulty and some loss in reliability) be fabricated on the same substrate with NPN units. A circuit representing a reasonable solution to this problem is shown in Fig. 3.13 The drive for this amplifier is assumed to be a single-ended PWM signal such as the output of the synchronous amplifier of Fig. 3.10. Notice the use of MOS field-effect transistors (p-channel depletion type) to provide the current drive to the top pair of transistors.

Diodes D_1 and D_2 provide the gating to alternately switch the top transistors depending on which one of the lower pair is conducting. Even though this circuit has not been completely evaluated it can be seen that the efficiency will be substantially lower than a push-push connection due to the fact that there are two transistors and one diode in series with the load. This could account for as much as a 13% loss in power output. It should be pointed out that the output impedance for the bridge circuit is in the 5 ohm range, and that this value would be somewhat higher in a monolithic design due to the top contact problem on the power transistor collector.

Other modifications to this circuit along the lines of a balanced drive for all four power transistors are now under consideration and will be presented in the final report. This drive could be obtained simply by adding a collector resistor to Q_9 of Fig. 3.10.

3.5.1 Microcircuit Practicality.

There is little question about the use of hybrid microcircuit construction as a practical way to fabricate either linear or switching amplifiers for low-pass loads such as those already memtioned. Hybrid techniques are better suited to the small-quantity production anticipated and in many cases the component tolerances can be better controlled. Furthermore, the breadboarding job is vastly simplified. However, the designs undertaken on this grant have been directed toward a monolithic approach which, it is felt, represents the best realization for space electronic systems.

The question of manufacturing feasibility for the most complex configuration presented here can be answered by considering two restrictions: (a) power dissipation,

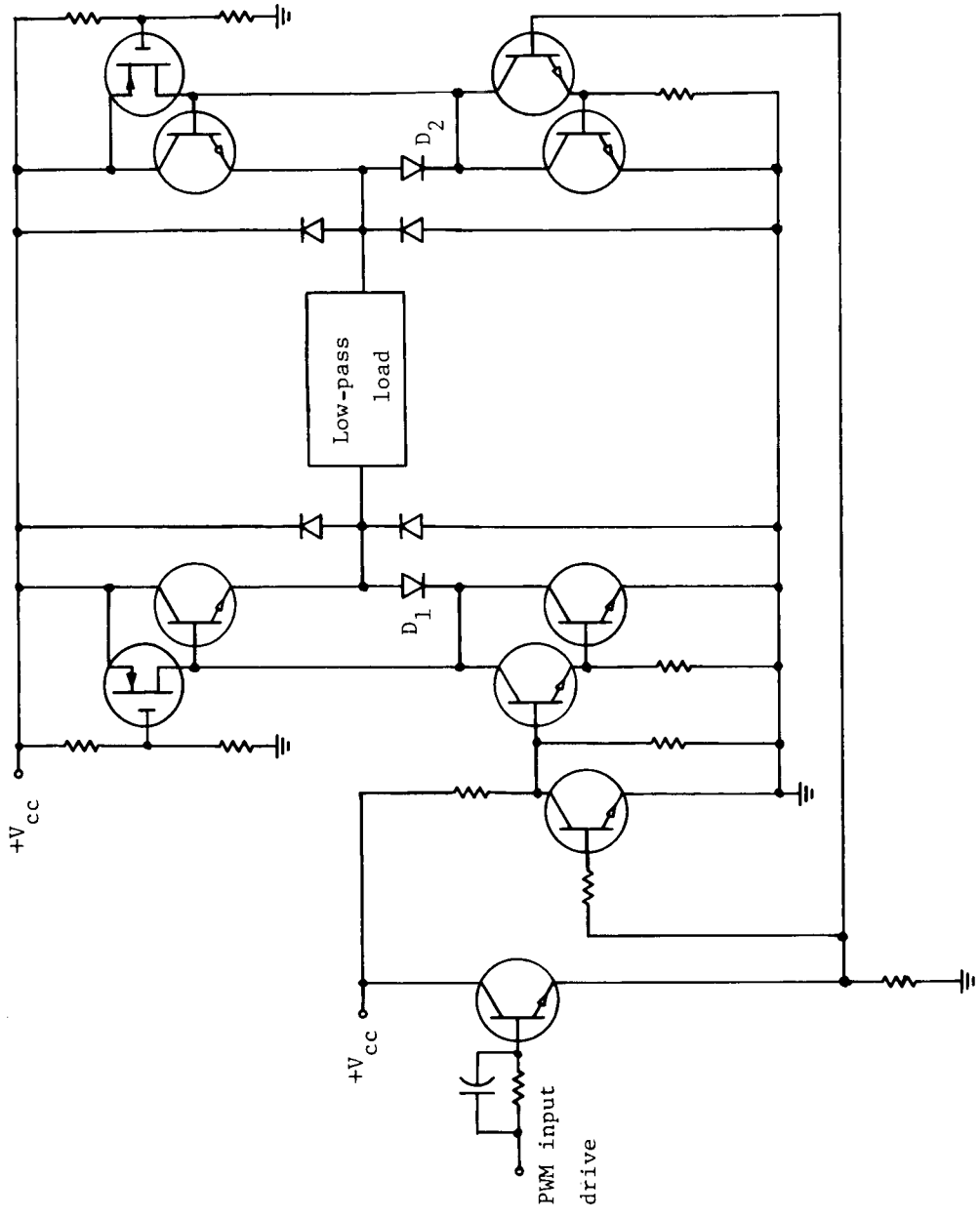

Fig. 3.13 Possible monolithic power stage (bridge).

(b) chip size. Assuming the worst efficiency to be 75%, the 2 watt amplifier would require that the package be capable of dissipating 0.5 watts at elevated temperatures. This can be done with a well heat-sinked TO-5 case.

Reference to Table 3.1 shows a reasonable component vs. chip area relationship for present-day technology in monolithics. The areas presented include the isolation space around the components. With this table, calculations for the synchronous modulator of Fig. 3.10 and power stage of Fig. 3.13, indicate the need for an area of about 6000 $mils^2$ (chip size of 60 x 100 $mils^2$). This is not at all unreasonable. It is interesting to note that roughly 2/3 of the area is taken up by the capacitors and power transistors.

There are, of course, many other subtle problems in microcircuit design which must still be considered but there is nothing deemed insurmountable. In fact, it is hoped that at least one of the switching amplifier designs presented in this chapter can be realized in monolithic integrated form before the end of this grant period.

TABLE 3.1

AREA OF INTEGRATED COMPONENTS

TYPE	SPECIFICATION	CHIP AREA (INCLUDING ISOLATION)
Diode	(10 mA)	17 mils^2
Transistor	A (10 mA, 20Ω)	32 mils^2
	B (10 mA, 15Ω)	120 "
	C (400 mA, 2Ω)	600 "
	D (1200 mA, 2Ω)	1200 "
Resistor	(± 20%)	
	100Ω	6 mils^2
	300Ω	7 "
	600Ω	9 "
	1kΩ	12 "
	2kΩ	20 "
	3kΩ	28 "
	5kΩ	45 "
	10kΩ	86 "
Capacitor (50 V)	100 pf	460 mils^2

Resistor pathwidth = (0.8 mil)

Minimum spacing between components = (0.4 mil)

ρ_s(Sheet resistivity) = 150Ω/□ (base region)

TABLE 3.2

COMPARISON OF DIFFERENT TYPES OF
SWITCHING AMPLIFIERS

TYPE	f_o(kc)	f_m(kc)	Modulation (%)	A_v*	Distortion(%)**
1	250	140	90	1.8	1.6
2(a)	330	120	90	3.5	5.6
2(b)	330	250	90	2.4	1.6
3(a)	250	250	90	5.1	5.7
3(b)	250	250	90	1.8	1.5
3(c)	250	250	90	5.3	2.0
4	280	100	85	2.4	4.8
5(a)	200	200	90	16.5	1.2
5(b)	200	200	90	16.5	5.5

1 - "T_d" amplifier with 1.2 V deadband
2(a) - Same as 1 with switched feedback
2(b) - Same as 2(a) with signal feedback
3(a) - Open loop with square-wave drive for RC
3(b) - Same as 3(a) with signal feedback
3(c) - Same as 3(a) with switched feedback
4 - Hysteresis Amplifier with 1.2 volts of hysteresis
5(a) - Synchronous modulator with sawtooth
5(b) _ Same as 5(a) with "hum bucking" circuit.

NOTE:

*Small signal including power stage

**Corrected for source distortion and not including ripple at switching frequency.

IV. Reliability Considerations

4.1 Conventional Reliability Theory.

The conventional approach to reliability theory is based on probability theory and is usually binary in nature. The individual elements have only two states: operational or failed, and the overall system has likewise only two states: satisfactory and non-satisfactory. Arbitrary limits are set on the performance of individual components, above which they are said to be good and below which they are said to have failed. In the simplest form of the theory (non-redundant) it is considered that the system fails whenever a component fails. A great deal of judgement is therefore required to determine the degree of component variation that constitutes a failure.

The simplest form of reliability theory assumes an exponential curve for reliability,

$$R(t) = \varepsilon^{-\lambda t} \quad , \qquad (4.1)$$

where R(t), (the reliability) is the probability of a device operating for time t and λ is the failure rate (a constant number).

In a series system (defined as one in which a failure of any one component causes a failure of the whole system)

$$R_s = \varepsilon^{\Sigma\lambda_i t} \quad , \qquad (4.2)$$

where $\Sigma\lambda_i$ is the sum of the failure rates of all the components. This formula is widely used in practice to obtain overall system failure rates (and the reciprocal of the failure rate, the mean time between failure).

For a parallel system (defined as one with redundant elements in parallel) it is more convenient to work with the unreliability

$$Q(t) = 1 - R(t) \quad . \qquad (4.3)$$

The unreliability of the parallel system is

$$Q_p = (1 - \varepsilon^{\lambda_1 t})(1 - \varepsilon^{\lambda_2 t})(1 - \varepsilon^{\lambda_3 t})\ldots \quad , \qquad (4.4)$$

where λ_i is the component failure rate, and the corresponding reliability is

$$R_p = 1 - Q_p = 1 - (1 - \varepsilon^{\lambda_1 t})(1 - \varepsilon^{\lambda_2 t})(1 - \varepsilon^{\lambda_3 t})\ldots \quad . \qquad (4.5)$$

As can be seen from this formula the reliability of a parallel or redundant system is much greater than that of a non-redundant or series system. A simple extension can be made to include series-parallel systems.

4.2 Reliability Based on Performance Degradation.

For many problems a binary type of reliability theory is not a satisfactory one. In fact, a whole new theory is needed in which some aspect of the performance of an overall system is successively degraded, rather than the whole system failing. Such a theory requires the presence of many redundant elements (as for example in the human brain) and probably was not required before the advent of microelectronics. It seems to be a prerequisite, however, for the rational design of microelectronic systems. Several possible performance criteria lend themselves to successive degradation by component failure.

The first and most obvious criterion is the power output. If there are several elements in parallel in the output of an amplifier the failure of one of them simply reduces the available power output. A more sophisticated form of this concept is the feedforward circuit (Sect. 4.4) in which the failure of any one channel merely reduces the peak power available.

A second performance criterion which can be subjected to successive degradation is the bandwidth. In a digitally sampled system, the bandwidth is a function of the sampling rate. If the sampler is designed so that each sampling pulse comes from a separate element, the failure of any one of them will merely decrease the overall bandwidth of the system.

A cursory analysis of the reliability problem makes it probable that the basic circuits should be digital in form and that they should be interconnected in complicated feedback and feedforward configurations. Indeed, it seems probable that the principal design criterion for microelectronic circuits may be the circuit, as opposed to the component, reliability.

4.3 Redundancy: Majority Voting.

One method of employing redundancy for the process of control is illustrated

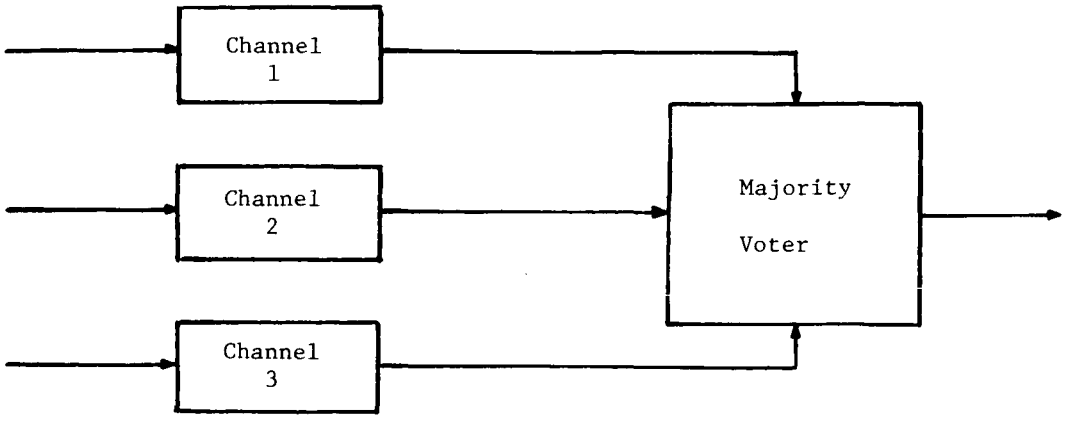

Fig. 4.1 Majority voting system

in Fig. 4.1. This system has the capability of operating without degraded performance with a failure of any type in any one of the three channels. A system with this characteristic is referred to as fail-operational. This feature is achieved by the majority voting circuit which selects the signal existing in two of the three channels at the proper control signal and rejects the third signal if it is different. It can be shown that the probability of failure for such a system is approximately

$$Q_R = 3Q^2 + Q_M \quad , \qquad (4.6)$$

where Q is the probability of failure of a single channel and Q_M is the probability of failure of the majority voting circuitry. Neglecting, for the moment, the effects of Q_M, it is clear that this technique achieves a remarkable improvement in system reliability. For example, if the probability of failure of a single channel is one in a thousand, then the system probability of failure is three in a million. This is because at least two channels of the three must fail in order to have a system failure. In order for Q_M not to substantially degrade the system reliability it must not be greater than approximately Q^2. If the majority voting is performed with digital logic, the circuitry is relatively simple. Despite this simplicity, it may have a probability of failure significantly higher than Q^2. Consequently, triple redundancy may be required in the digital logic circuitry so as not to impair system reliability.

4.4 Redundancy: Analog.

A triple-redundant analog scheme, developed by Autonetics, and called TRISAFE*,

* Triple Redundancy Incorporating Self-Adaptive Failure Exclusion

is shown in Fig. 4.2. Automatic failure correction is achieved by making use of the analog amplifier voltage saturation characteristics in a high-gain loop with protected common-point feedback. A simple linear analysis of this amplifier configuration yields

$$e_o/e_i = - \frac{R_3 - 3R_2/(K_1 + K_2 + K_3)}{R_1 + 3(R_1 + R_2 + R_3)/(K_1 + K_2 + K_3)} \quad , \qquad (4.7)$$

which for very high unit gain(K_1, K_2, K_3), becomes

$$e_o/e_i = - R_3/R_1 \quad . \qquad (4.8)$$

The failure correction feature of TRISAFE has been termed self-adaptive because no measuring device outside of the triple unit, such as a majority voter, is required. In addition, according to Autonetics, a failure mode analysis shows that many types of double failures (two units out of three) do not degrade the triple unit operation.

A novel n-path feedforward amplifier system has been investigated during this report period. This system, shown in Fig. 4.3 not only has the feature of high reliability provided by redundant circuitry, but ideally affords an n-multiplication of the dynamic range of a single amplifier. If, for example, a signal is applied to a first amplifier that causes saturation, the difference signal ($e_i - e_1/A$) appears as the input of the second amplifier, is amplified and added to the output of the first. Note that this voltage is zero when there is no saturation <u>and</u> if $A_1 = A$ (nominally,

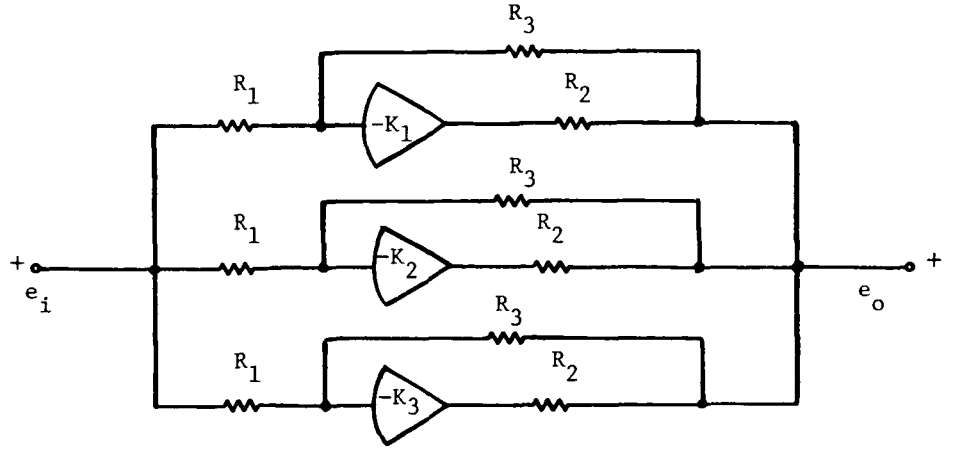

Fig. 4.2 TRISAFE scheme for reliable amplifier operation.

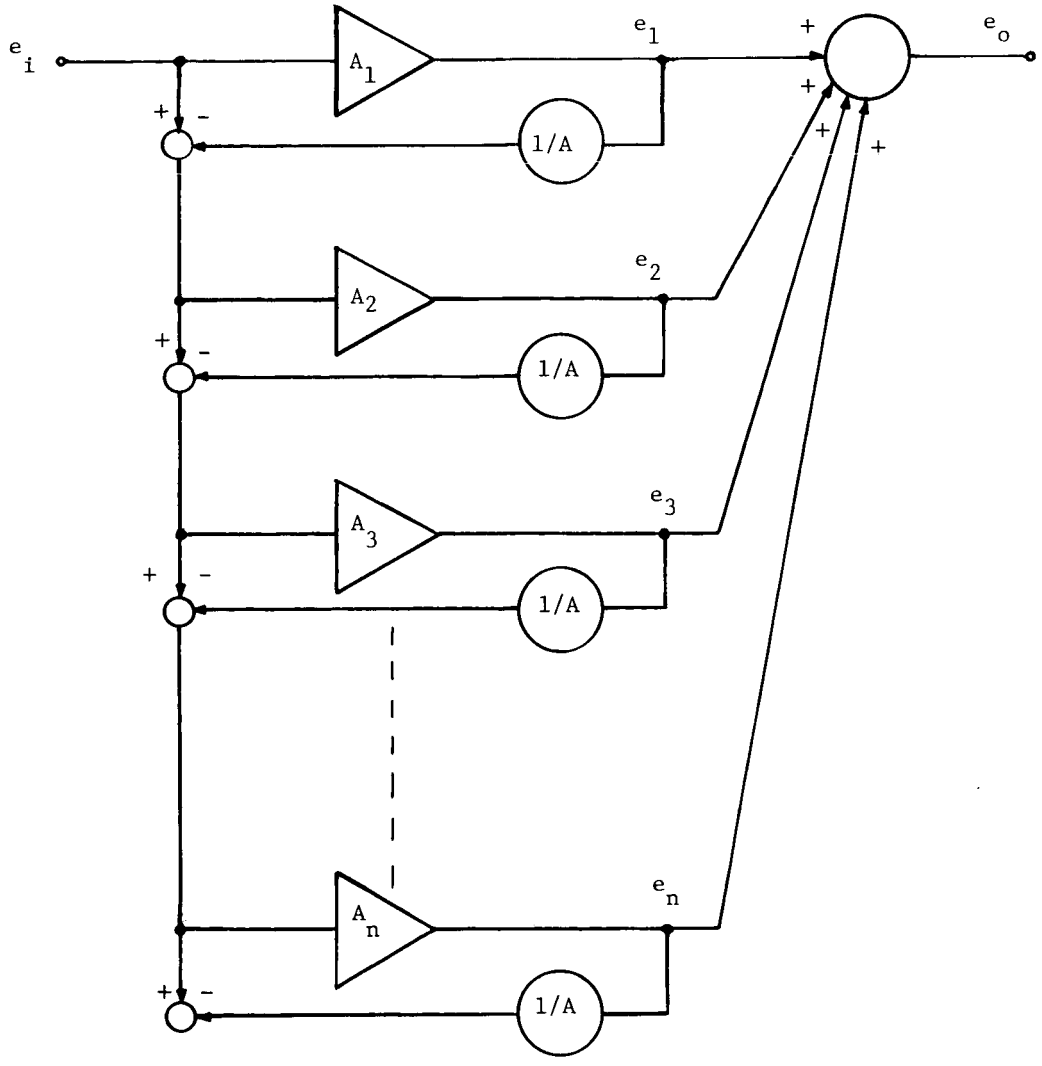

Fig. 4.3 Feedforward scheme for reliable amplifier operation.

$A_1 = A_2 = A_3 \ldots = A_n = A$). Subsequent units are similarly connected and the outputs are summed. This effect is illustrated in Fig. 4.4, where it can be seen that saturation in the first two amplifiers does not affect the output.

With the feedforward system, if any amplifier should fail the only degradation in performance is a reduction of 1/n in dynamic range. In addition, if all amplifiers should drift from the nominal gain A by the same amount Δ, the change in system gain (also nominally A) is approximately $(\Delta/A)^n$ for small Δ. To illustrate, a detailed three-operational amplifier feedforward system is shown in Fig. 4.5. With reference to the diagram it can be seen that

$$e_1 = - A_1 e_i \quad , \tag{4.9}$$

$$e_2 = -A_2(1 - A_1/A)e_i \quad , \tag{4.10}$$

$$e_3 = -A_3[1 - A_1/A - (A_2/A)(1 - A_1/A)]e_i \quad , \tag{4.11}$$

and that

$$e_o = e_1 + e_2 + e_3 \quad . \tag{4.12}$$

Inspection of (4.9) and (4.10) reveals that if $A_1 = A_2 = A$, $e_2 = e_3 = 0$ and $e_o = - Ae_1$. Deviation of gain from the value A is compensated for by the redundancy. For example, if $A_1 = A_2 = A_3 = A + \Delta$, from (4.9), (4.10), (4.11), and (4.12), the system gain may be characterized by the expression

$$T + \Delta T = -[3(A + \Delta) - 3(A + \Delta)^2/A + (A + \Delta)^3/A^2] \quad , \tag{4.13}$$

where T is the transfer ratio

$$T = e_o/e_i\Big|_{A_1 = A_2 = A_3 = A} \quad , \tag{4.14}$$

and ΔT is the deviation of that ratio from the nominal value A. Hence, from (4.13) the fractional change in the transfer ratio is

$$\Delta T/T = (\Delta/A)^3 \quad . \tag{4.15}$$

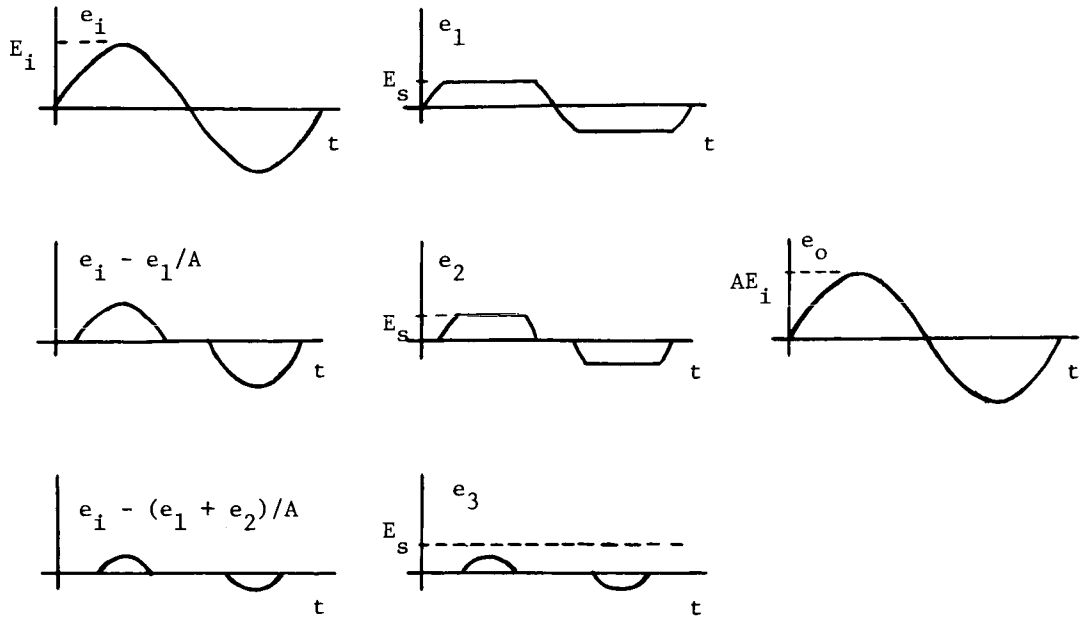

Fig. 4.4 Operation of feedforward configuration when the amplifiers saturate.

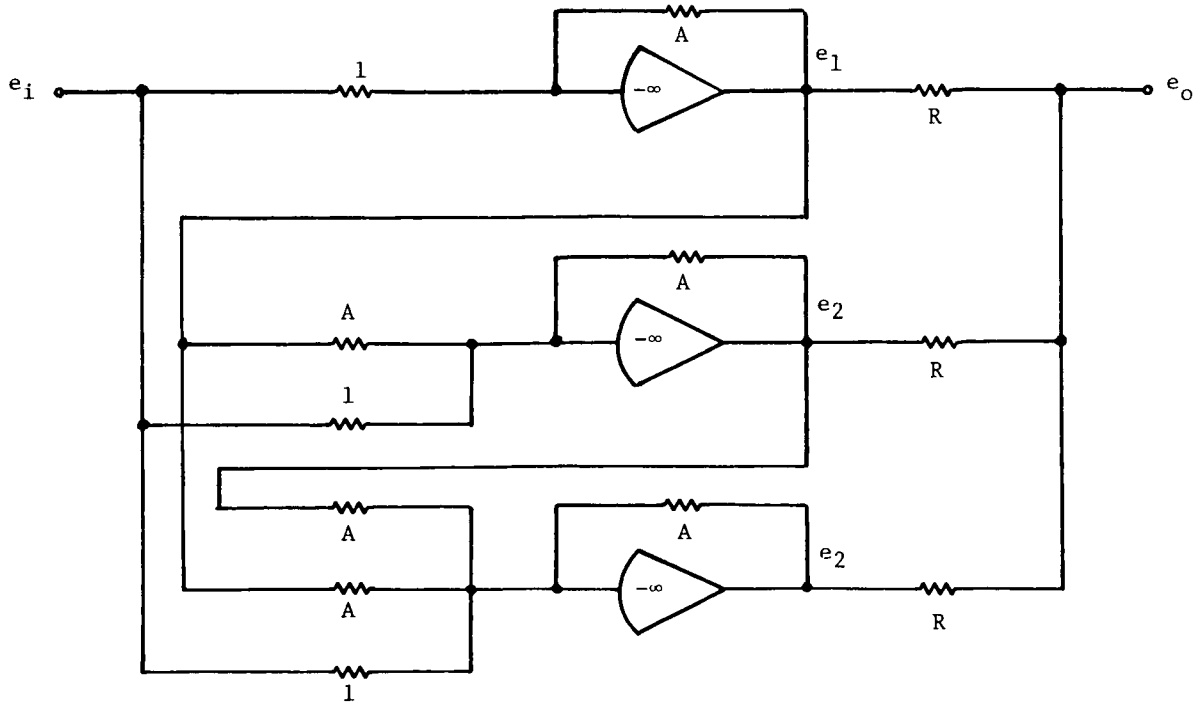

Fig. 4.5 Three-amplifier analog computer representation of feedforward scheme.

In summary, it has been shown that the feedforward configuration provides reliability through redundancy, dynamic range extension and the advantages of negative feedback in maintaining the transfer ratio insensitive to parameter changes. In addition, it seems feasible to split the frequency band of a signal to be amplified and use amplifier sections appropriate to the power and frequency requirements of each of the sub-bands. The possibilities of the method are quite exciting both for use with ordinary linear amplifiers and with switching amplifiers. Attention is being given to the development of practical applications of the feedforward method.

V. Conclusions and Research Plans.

The research discussed in this report has been directed toward the application of advanced circuit concepts for realization of highly reliable and efficient electronic subsystems. Many of the conclusions resulting from the first six months of grant research are of a tentative nature; however, they form the basis for a continuing research effort in the area of reliable solid-state circuits. The main conclusions, with suggestions for future work, are as follows:

(1) The operation of a two-state modulator with hysteresis and RC feedback has been shown to be equivalent to the operation of an astable multivibrator (Appendix A).

(2) A theoretical development of the operating characteristics of a two-state modulator with switched RC feedback has been given. Comparison with the simple RC feedback modulator has demonstrated that the modified system exhibits less variation in switching period, has a higher gain and a more linear transfer characteristic. (Chapter II). Experimental results have generally verified this conclusion (Chapter III), although, from a practical viewpoint, a new design, not discussed in this report, shows greater promise (see 5(a), below).

(3) The self-oscillating switching designs described in Chapters II and III include the signal in the feedback path. On the basis of the work reported here, it would appear desirable to eliminate the signal from the switching loop and provide separate signal feedback for linearity improvement. The feasibility of this approach will be investigated.

(4) It is well-known that a linear-transfer characteristic can be obtained from a switching amplifier if a perfect triangle or a linear sawtooth is used as a switching waveform. However, results of an analysis of a synchronous modulator with exponential segments for a switching waveform show surprisingly small nonlinearity (Chapter II). Investigation leads to the conclusion that a switching waveform having symmetrical segments tends to be self-compensating, indicating that if a triangular wave is used, highly linear segments are not necessary. On the other hand, a nonlinear transfer characteristic (a logarithmic relation, for example) should be obtainable by suitably shaping a sawtooth waveform. Further investigation of these properties is anticipated.

(5) An important conclusion based on the designs presented in Chapter III is that practical realization of a PWM power amplifier combining the features of high

reliability, high efficiency and low distortion is entirely feasible and further, is compatible with the requirements of present-day integrated circuit technology. Research will continue in the area of switching amplifier design with special attention given to the following:

(a) Development of a self-oscillating, constant switching-frequency design with high gain and low distortion.

(b) An investigation to determine the magnitude of switching losses for practical inductive loads.

(c) Introduction of MOS-FETs for high input impedance and improved switching characteristics.

(d) All NPN power-stage design in a bridge configuration. The use of MOS-FETs here may realize the benefits of complementary operation in a form easily integrated.

(6) In the area of reliability theory, it is felt that a measure of system degradation (as a function of component failure) would be very useful in the study of large-scale systems (Chapter IV). Supporting research will be carried towards this goal.

(7) It has been shown that a novel feedforward amplifier configuration provides reliability, extension of dynamic range and the advantages of negative feedback. Further research effort will be directed to development of practical applications of the method, including the realization of switching amplifiers in the configuration.

(8) Two applications of the unijunction transistor for amplitude regulation of an RC oscillator have been described (Appendix B). Very recent publications indicate, however, that field-effect devices may be equally suitable for this application.

VI. References.

[1] Carlson, A. W., Scientific Report No. 6, Contract No. AF19(604)-4089, May 1961, Transistor Applications, Inc., Boston, Massachusetts.

[2] Bedford, B. D., "Improvements in and Relating to Electric Amplifying Circuits", U. K. Patent No. 389,855, March 1933.

[3] Watts, R. J. "Pulse-Width Modulation", U. S. Patent No. 2,556,457, June 1951.

[4] Bose, A. G., "A Two-State Modulating System", Electro-Technology, August, 1964, pp. 42-47

[5] Loos, C. H., "Time Proportional Control", Control Engineering, May, 1965, pp. 65-70

[6] Clark, L., "New Unijunction Geometries", Electronics, June 14, 1965, pp. 93-97.

APPENDIX A

Comparison of Two-State Modulator and Multivibrator Operation

The two-state modulator shown in Fig. A.1 has been described by Bose [4]. It is here demonstrated that the system operation is equivalent to that of an astable multivibrator with a modulating signal injected. The notation used in the derivation is the same as that used by Bose in his paper.

A.1 System Operation.

In the modulator in Fig. A.1 when the signal x, the sum of the modulating signal s and the feedback signal f, exceeds the value w_1, the output y assumes the level h_2. It remains there until x becomes less than w_2 at which point y switches to h_1. The operating point in the x-y plane follows the path indicated by the arrows.

The system is designed to oscillate producing a rectangular waveform at the output having a period of T_o in the absence of an input signal. The input signal alters the frequency and duration of the output pulses in such a way that the average value of the output is a replica of the time-varying input signal which may then be recovered by low-pass filtering. The bandwidth of the input signal must be limited to some small fraction of the lowest switching frequency dependent upon the allowable distortion.

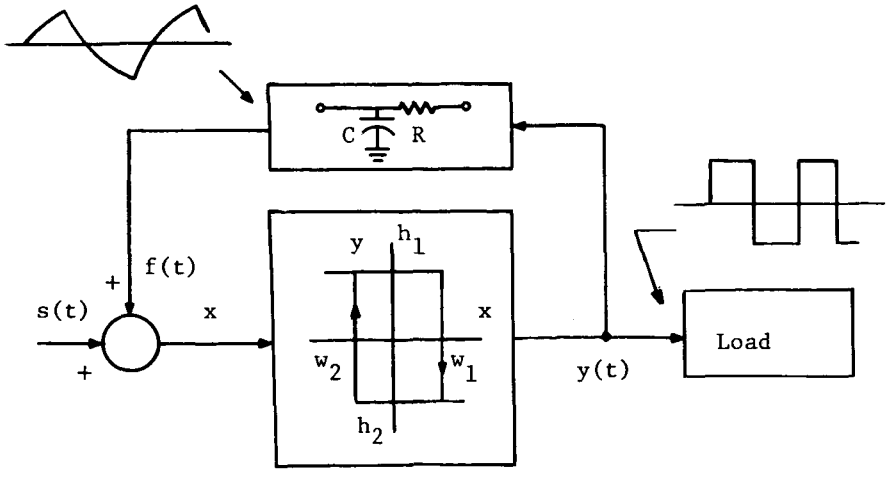

Fig. A.1 Block diagram of two-state modulator.

Bose has made an analysis of this modulator for the case where the feedback consists of a single time-constant network cascaded with a delay element. Thus, the unit-step response of the feedback circuit is taken as $1 - \varepsilon^{-(t - T_d)/\tau}$ for $t > T_d$, and zero for $t < T_d$, where T_d is the time delay and τ is the time constant of the feedback circuit. The effect of T_d is to cause x to overshoot the w_1, w_2 switch points.

The details of Bose's analysis will not be duplicated here. He has calculated the time intervals for each of the two states of the output, the switching period, and the average value of the output signal as a function of the input signal and system parameters. The results he obtained for the case of symmetrical hysteresis are sufficient for present purposes.

For the case of symmetrical hysteresis, $h_1 = -h_2 = h$ and $w_1 = -w_2 = w$, Bose derives the following:

$$\bar{y} = \frac{h \ln[(R + N)(1 - N)/(R - N)(1 + N)]}{\ln[(R + N)(R - N)/(1 + N)(1 - N)]} \quad , \qquad (A.1)$$

$$T_2 = \tau \ln[(R^2 - N^2)/(1 - N^2)] \quad , \qquad (A.2)$$

and $$T_0 = 2\tau \ln R \quad , \qquad (A.3)$$

where R and N are defined as follows:

$$R = 2h\varepsilon^{T_d/\tau} - 1 \quad , \qquad (A.4)$$

$$N = s/(h - w) \quad . \qquad (A.5)$$

In the above, $\bar{y}$ is the average value of the output signal and represents the useful output of the system as an amplifier. T_2 is the period of the output pulses with s, the input signal, equal to zero.

A.2 Equivalent Multivibrator.

The equivalence between Bose's system and an astable or freerunning multivibrator will be shown by considering an astable multivibrator controlled by a single reactive element which for convenience is taken to be a capacitor (Fig. A.2). The ca-

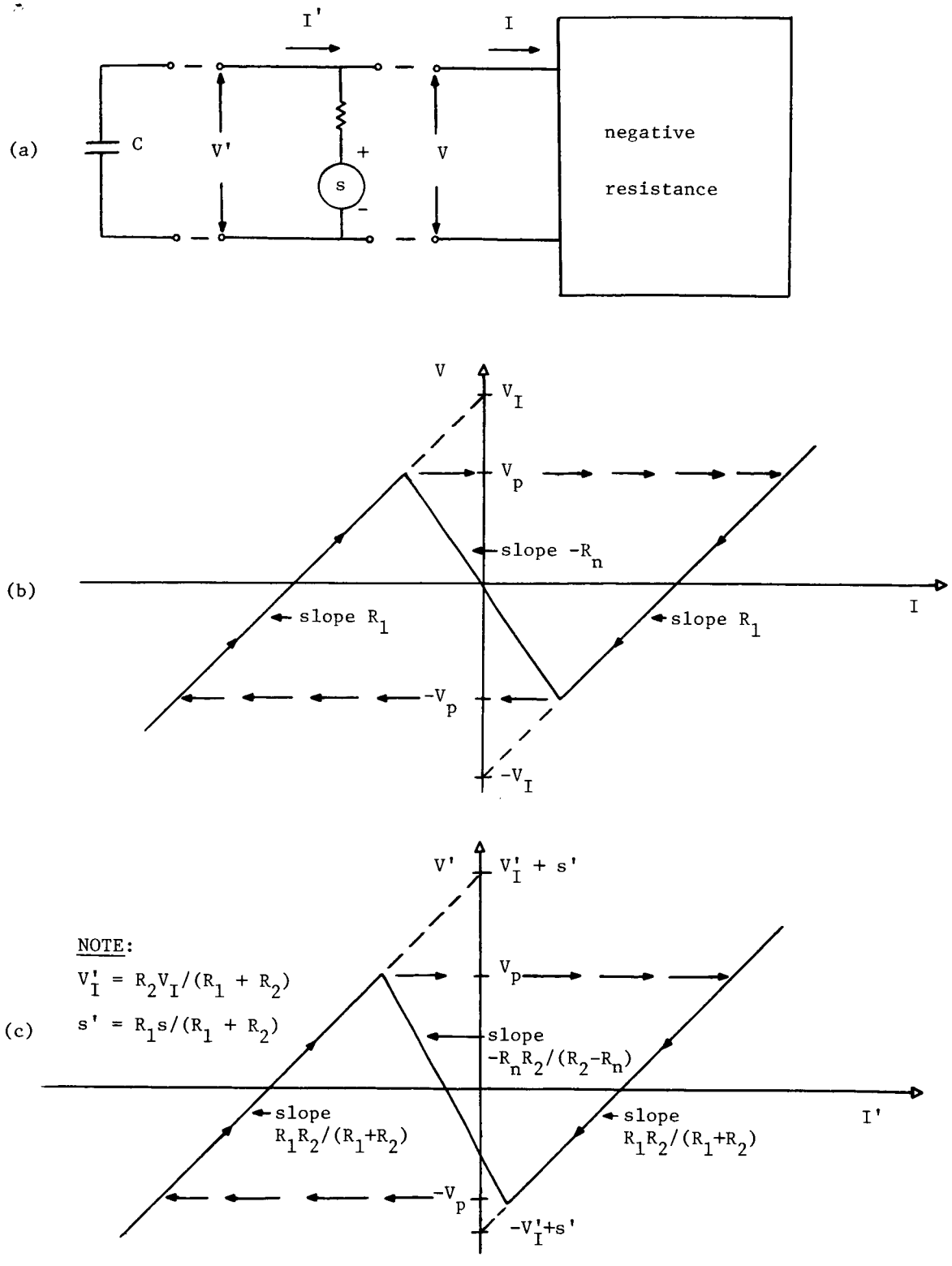

Fig. A.2 (a) Astable multivibrator with modulation. (b) Multivibrator V-I characteristic (s = 0). (c) Multivibrator V' - I' characteristic (with modulation).

pacitor sees at its terminals a negative resistance of the open-circuit stable or N type. To correspond to Bose's symmetrical hysteresis case the negative resistance characteristic will be assumed to be symmetrical, i. e., the peak and valley voltages will be of equal magnitude and in the positive resistance regions the slopes will be identical and the intercept voltages equal in magnitude. This symmetrical multivibrator characteristic is shown in Fig. A.2(b) with the path of the operating point in the V-I plane marked by arrows.

The multivibrator may be modulated by applying a signal so as to modify the negative resistance characteristic seen by the capacitor as shown in Fig. A.2(c). The V' - I' characteristic is obtained by combining the series combination s and R_2 in parallel with the V-I characteristic. The peak and valley voltages are unchanged in going from the V-I plane to the V' - I' plane but the slopes and intercept voltages are modified. The effect of the signal s is to alter the intercept voltages of the V' - I' characteristic and to cause it to shift left or right along the I' axis in accordance with the polarity and magnitude of signal s.

Let T_1 be the time that the operating point is on the left hand side of the V' - I' curve in Fig. A.2(c), T_2 be the period of oscillation of the multivibrator, and τ be equal to $R_1R_2C/(R_1 + R_2)$, the time constant of the oscillator.

From inspection of Fig. A.2(c) it can be seen that

$$T_1 = \tau \ln[(V_I' + V_p + s')/(V_I' - V_p + s')] \quad , \qquad (A.6)$$

by noting that the voltage across the capacitor is initially at $-V_p$ when the operating point switches to the left side and increases exponentially toward a final value $(V_I' + s')$ but switches to the right side at T_1 when the voltage reaches V_p. That is, the voltage across the capacitor while the operating point is on the left side is $(V_p + V_I' + s')(1 - \varepsilon^{-t/\tau}) - V_p$ with t = 0 the moment of switching to the left side.

Similarly, the time that the operating point is on the right side of the characteristic is given by

$$T_2 - T_1 = \ln[(V_I' + V_p - s')/(V_I' - V_p - s')] \quad . \qquad (A.7)$$

The period of oscillation is obtained by adding equations (A.6) and (A.7) to obtain

$$T_2 = \tau \ln\{[(V_I' + V_p)^2 - (s')^2]/[(V_I' - V_p)^2 - (s')^2]\} \quad . \qquad (A.8)$$

To bring the notation into agreement with that of Bose let

$$R = (V_I' + V_p)/(V_I' - V_p) \quad , \tag{A.9}$$

$$N = s'/(V_I' - V_p) \quad . \tag{A.10}$$

Substitution of (A.9) and (A.10) into (A.6),(A.7) and (A.8) yields

$$T_1 = \tau \ln[(R + N)/(1 + N)] \quad , \tag{A.11}$$

$$T_2 - T_1 = \tau \ln[(R - N)/(1 - N^2)] \quad , \tag{A.12}$$

$$T_2 = \tau \ln[(R^2 - N^2)/(1 - N^2)] \quad . \tag{A.13}$$

Equation (A.13) is seen to be identical to (A.2) derived by Bose.

Suppose that the multivibrator produces an output signal $\bar{y}$ (either by itself or by controlling a suitable switch) that has the value h during the interval T_1 and the value -h during the interval $(T_2 - T_1)$. Then

$$\bar{y} = \frac{hT_1 - h(T_2 - T_1)}{T_2} = \frac{h \ln[(R + N)(1 - N)/(R - N)(1 + N)]}{\ln[(R + N)(R - N)/(1 + N)(1 - N)]} \quad , \tag{A.14}$$

where $\bar{y}$ is the average value of y. Equation (A.14) is seen to be identical to (A.1), and when N = 0 (no signal, s also zero), (A.13) becomes

$$T_o = T_2\Big|_{s = 0} = 2\tau \ln R \quad , \tag{A.15}$$

which is the same as (A.3) given by Bose.

Thus it has been demonstrated that Bose's system is equivalent to modulating an astable multivibrator, when the feedback contains a single time constant. The voltage V_p corresponds to w in Bose's system and the intercept voltage V_I' corresponds to h as far as determining time intervals is concerned. With these equivalents and identifying s' with Bose's s, (A.9) and (A.10) are the same as (A.4) and (A.5) when the time delay T_d is zero. Without the time delay considered by Bose, R is a measure

of the portion of the exponential used in generating the output pulses. When R is large a greater portion of the exponential is used and the nonlinearity of the response is increased. The parameter N represents a normalized signal, the modulation of the output signal being complete when the magnitude of N is unity.

A multivibrator described by a negative-resistance characteristic that has unequal peak and valley voltage magnitudes and unequal intercept voltage magnitudes corresponds to Bose's general case. If in addition, the slopes in the positive resistance regions are unequal the multivibrator becomes equivalent to what Bose's system would be if the feedback time constant were to have one value for one state of the output and a different value for the other state.

Appendix B

Oscillator Amplitude Regulation Using the Unijunction Transistor

B.1 Amplitude Regulation.

One purpose of automatic amplitude regulation of an oscillator is to maintain the output at a constant level independent of changes in circuit values, supply voltages, frequency, etc. over reasonable limits. A second important function is to limit operation to the linear region in order to minimize distortion in the output waveform.

An incandescent lamp is frequently used as an amplitude control device in RC oscillators (such as the Wien bridge oscillator). The lamp is placed in the circuit in such a way that an increase in oscillator signal amplitude causes the power dissipated in the filament to increase, the temperature to rise, and the filament resistance to increase. If the increase in lamp resistance acts to decrease the oscillator loop gain, the output of the oscillator can be stabilized at a point where oscillations of the desired amplitude are sustained. The lag in response of the filament temperature to a change in power dissipated acts as a filter; the lower frequency limit to the lamp's usefulness comes when the temperature variation over a cycle of oscillation results in an unacceptable amount of distortion.

It is the purpose of the discussion to demonstrate that the unijunction transistor may be used instead of the incandescent lamp for oscillator amplitude control. This device, in addition to providing more reliable operation, is easily integrated [6]. The following describes two distinct applications of the unijunction in solid-state oscillator circuits.

B.2 The Unijunction Transistor.

Fig. B.1 is a sketch of the V_{b2} - I_{b2} characteristics of a unijunction transistor with I_E as a parameter. It is seen that at low positive voltage the slope of the constant I_E curves changes appreciably with I_E; the incremental resistance in this region, over a range of about 0.4 volts, is a nearly linear, decreasing function of I_E. Above and below the breakpoints in the low voltage region the incremental resistance is higher and a decreasing function of I_E, but is not nearly so sensitive to I_E as in the low voltage region. Fig. B.2 shows a plot of incremental resistance for a 2N489 unijunction transistor over the linear portion of the low-positive voltage region. In the region beyond the breakpoints, the change in incremental resistance is very

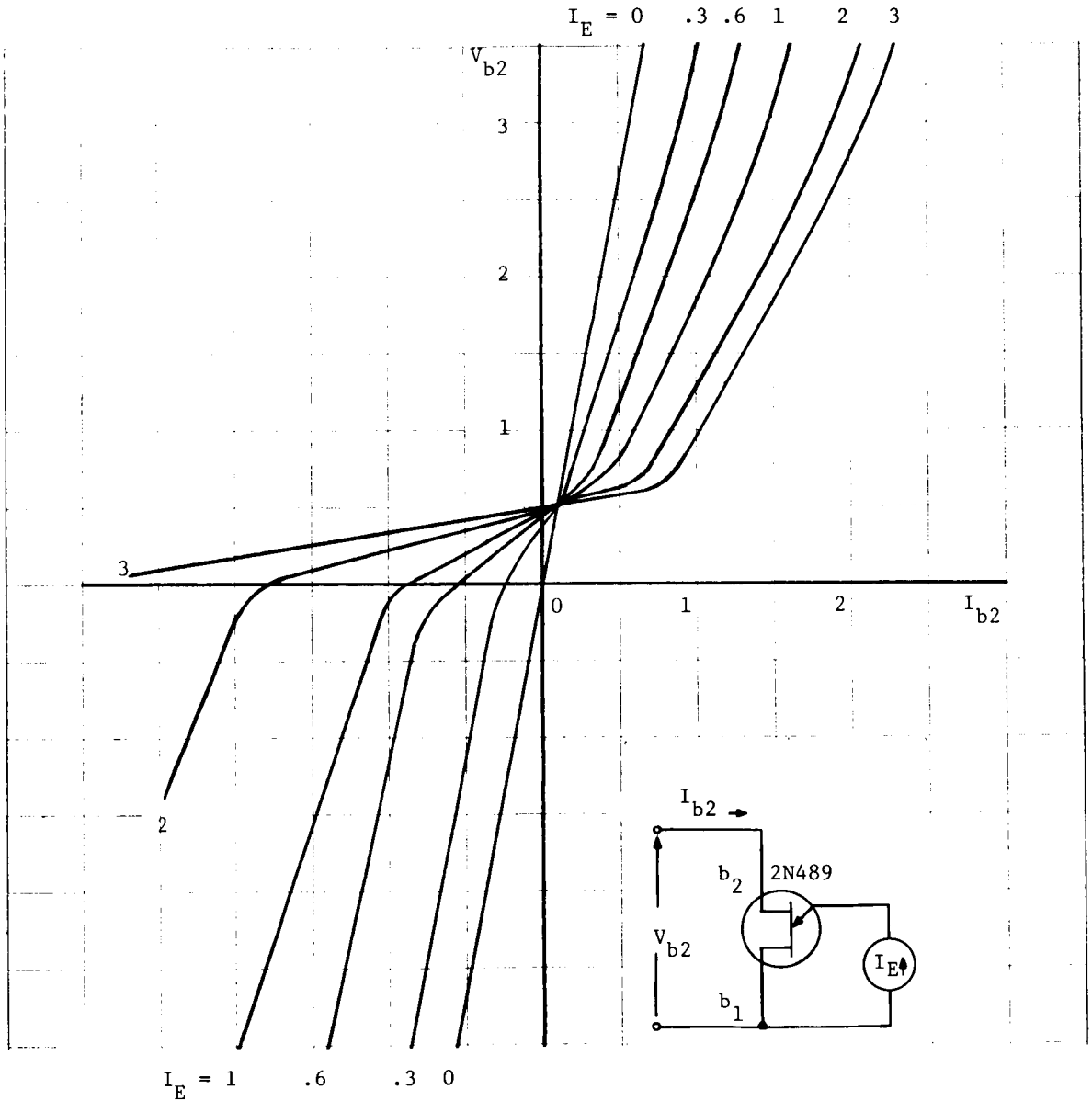

Fig. B.1 V_{b2} - I_{b2} Unijunction Characteristic.

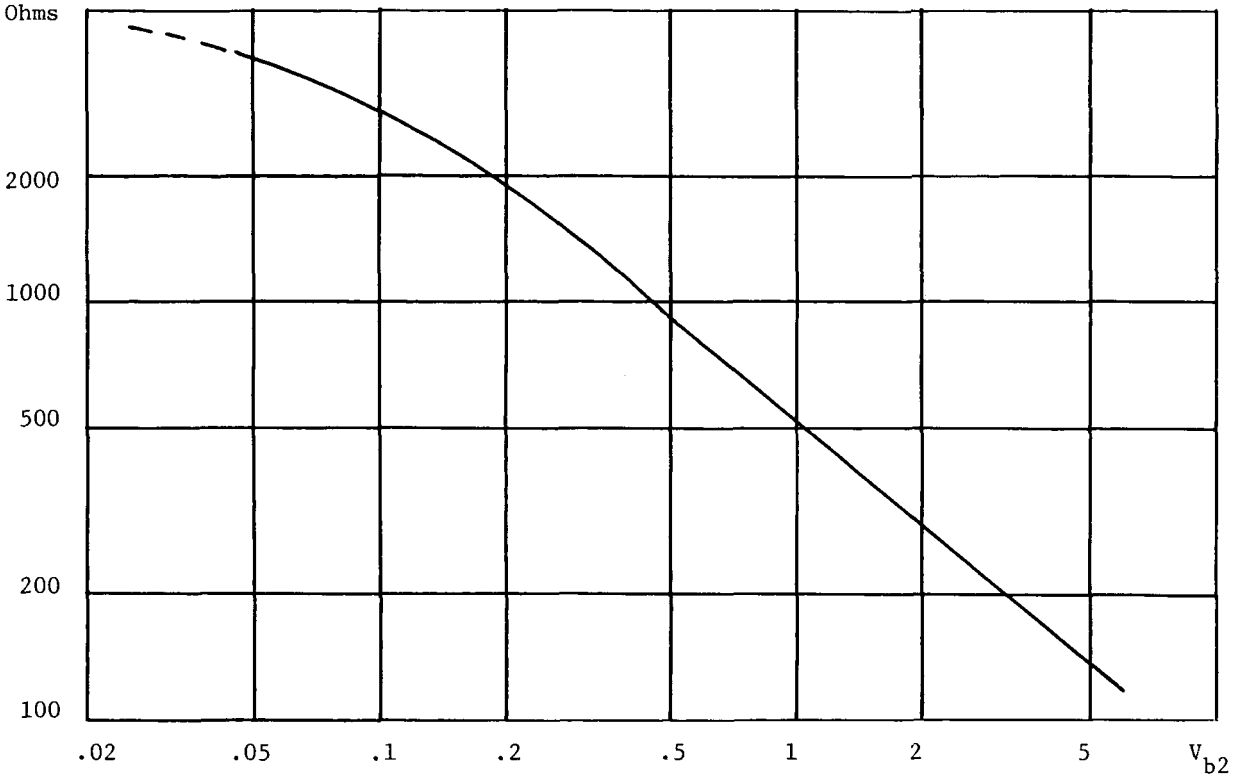

Fig. B.2 Incremental resistance vs. voltage (V_{b2}) for a 2N489 unijunction transistor

much less, perhaps a two-to-one variation over a range of I_E from 0 to 4 milliamperes.

The unijunction may be used to control amplitude in two different ways, by use of different portions of the V_{b2} - I_{b2} characteristics. Operation over the linear portion of the V_{b2} - I_{b2} curves in the low voltage region (between the breakpoints) is suitable for amplitude control with the unijunction located in that part of the circuit where gain is decreased by an increase in resistance (otherwise the gain would increase at the ends of the region being used and distortion would be extreme). Operation over that part of the V_{b2} - I_{b2} curves beyond the breakpoints (either quadrant) is suitable for amplitude control with the unijunction located in the circuit so that a decrease in resistance results in a gain reduction.

The unijunction transistor may be biased stably if the emitter current is supplied by a current source or a source having a resistance greater than the negative resistance seen at the emitter. The limited frequency response of the unijunction also permits an appreciable amount of shunt capacitance at the emitter without causing instability. The collector circuit of a transistor is a suitable source of emitter current bias for operating a unijunction as an amplitude control element.

B.3 Oscillator Circuits.

Fig. B.3(a) shows a feedback amplifier typically used in the Wien bridge oscillator shown in Fig. B.3(b). This circuit was employed to test the operation of the unijunction transistor as an amplitude control element. The amplifier has a high input resistance, a low output resistance, and a voltage gain of approximately $(1 + R_2/R_1)$. In the oscillator circuit of Fig. B.3(b), when $R_s = R_p = R$ and $C_s = C_p = C$, an amplifier gain of 3 is required to sustain oscillation at frequency $1/2\pi RC$.

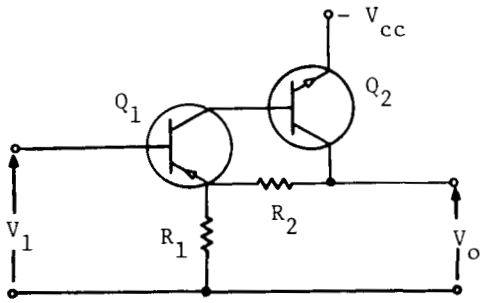

(a)

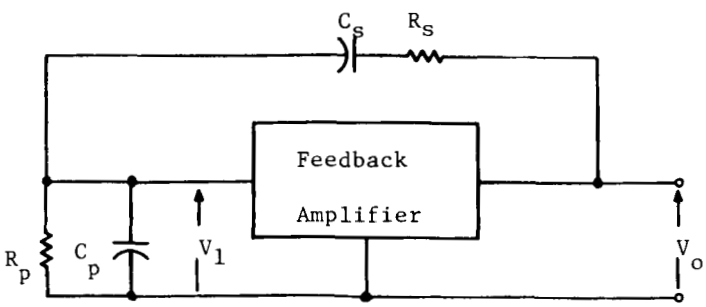

(b)

Fig. B.3 (a) Typical feedback amplifier used in (b) Wien-Bridge oscillator

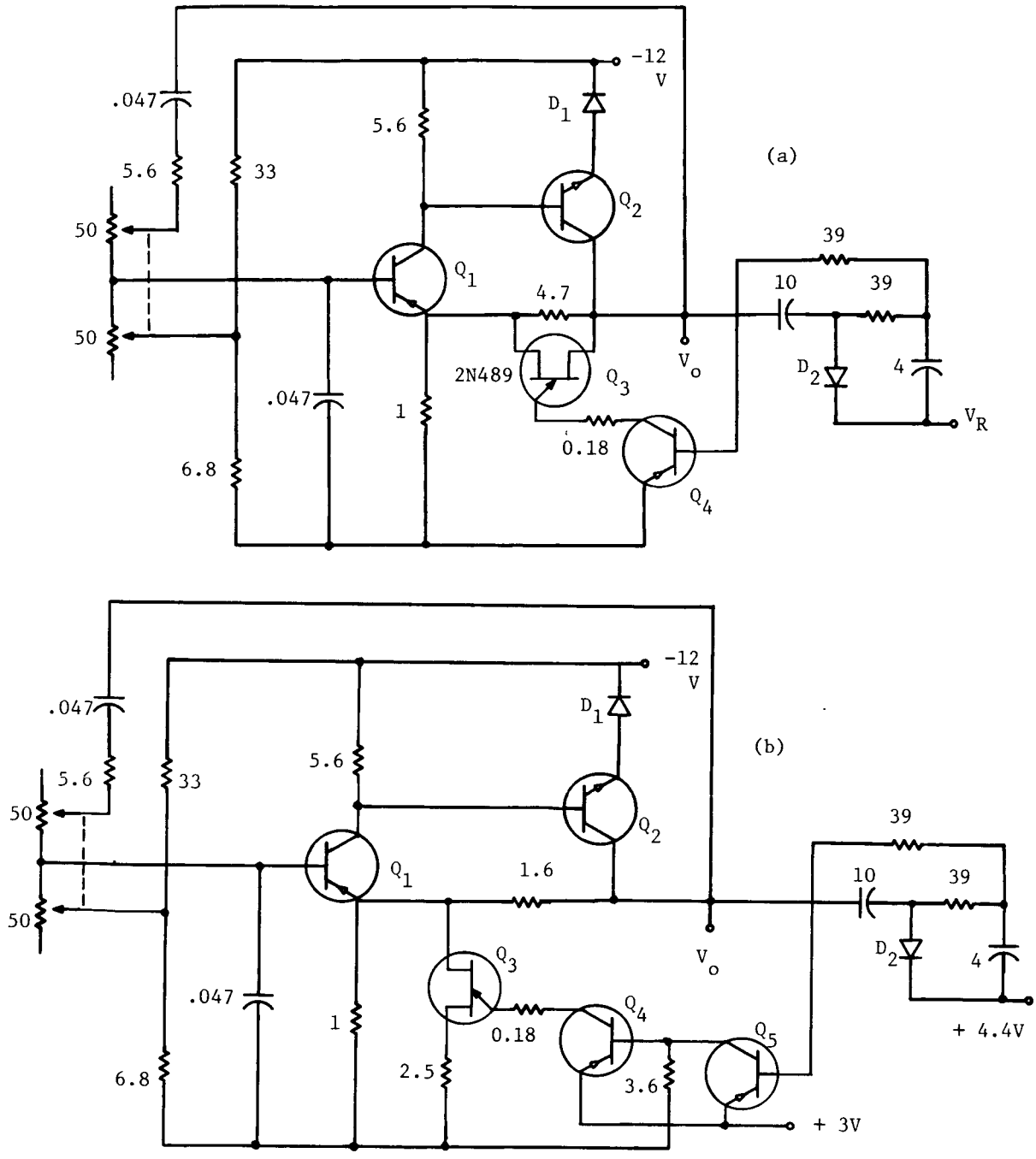

Note: All resistor values in kilohms, all capacitor values in microfarads

Fig. B.4 Wein-Bridge Oscillator circuits showing two ways of using unijunction transistors for amplitude control.

In Fig. B.4(a) and (b), two Wien-bridge oscillator circuits, adjustable by ganged potentiometers over the range of 60 to 600 cps. are shown. The circuits are essentially the same except for the manner in which the unijunction transistors are used to regulate oscillator amplitude. In each circuit, the output voltage is rectified, filtered and compared to a reference V_R (shown as 1.4 volts). This error signal is amplified to provide the emitter current needed by the unijunction transistor to maintain the amplitude constant. If the gain of the amplitude control loop is sufficiently high, the peak-to-peak amplitude of the oscillations equals $2V_R$, neglecting voltage loss in D_2 and V_{be} drops in control loop transistors. In the circuit of Fig. B.4(a), the peak-to-peak amplitude of the output was held constant at 4 volts, and in the circuit of Fig. B.4(b) at 6.4 volts, with V_R of 1.4 volts.

In Fig. B.4(a) the unijunction transistor is operated in the first quadrant above the breakpoints in the V_{b2} - I_{b2} curves and functions as part of resistance R_2 in the circuit of Fig. B.3(a). The emitter current supplied to the unijunction by Q_4 in accordance with the error signal must increase to reduce the gain (for amplitude regulation) of the amplifier.

In Fig. B.4(b) the unijunction is operated in the low voltage region between the breakpoints of the V_{b2} - I_{b2} curves shown in Fig. B.1 and is connected to form part of resistance R_1 in the amplifier of Fig. B.3(a). Here the emitter current supplied to the unijunction must be reduced by the error signal to reduce amplifier gain and oscillator output.

The unijunction transistor functions equally well in both methods of control shown in Fig. B.4. With 2N489 transistors the B1 and B2 connections can be interchanged with little change in operation except that in the circuit of Fig. B.4(a), the emitter current level in the unijunction approximately doubles.